

Sensor and Simulation Notes

Note 288

12 September 1985

LUMPED ELEMENT NETWORKS FOR REPLACING
SECTIONS OF A BURIED TRANSMISSION LINE

Y.-G. Chen, R. Crumley and S. Lloyd
Maxwell Laboratories, Inc., San Diego, CA

Carl E. Baum
Air Force Weapons Laboratory

and

D.V. Giri
Pro-Tech, 125 University Avenue, Berkeley CA 94710

Abstract

A buried transmission line formed by vertical conductors, can function as a wave guiding structure, in producing a part of the electromagnetic field distribution caused by a distributed source at the air-earth interface. Such a structure, when excited by an appropriate low-frequency source is a viable EMP simulation technique for use with underground systems. In the developmental phase of such a technology, there exists a need to artificially elongate the buried line by using lumped element networks. In effect, such networks simulate the simulator plates and earth and, perhaps are useful in the actual site of a large buried structure as well. This note addresses such a network concept and its design considerations. The actual design, fabrication and testing of an example network is also presented.

Approved for public release; distribution unlimited.

~~SECRET~~
CLEARED FOR PUBLIC RELEASE

PL/PA 15 JAN 97

PL 96-1148

Sensor and Simulation Notes

Note 288

12 September 1985

LUMPED ELEMENT NETWORKS FOR REPLACING
SECTIONS OF A BURIED TRANSMISSION LINE

Y.-G. Chen, R. Crumley and S. Lloyd
Maxwell Laboratories, Inc., San Diego, CA

Carl E. Baum
Air Force Weapons Laboratory

and

D.V. Giri
Pro-Tech, 125 University Avenue, Berkeley, CA 94710

Abstract

A buried transmission line formed by vertical conductors, can function as a wave guiding structure, in producing a part of the electromagnetic field distribution caused by a distributed source at the air-earth interface. Such a structure, when excited by an appropriate low-frequency source is a viable EMP simulation technique for use with underground systems. In the developmental phase of such a technology, there exists a need to artificially elongate the buried line by using lumped element networks. In effect, such networks simulate the simulator plates and earth. This note addresses such a network concept and its design considerations. The actual design, fabrication and testing of an example network is also presented.

CLEARED
FOR PUBLIC RELEASE
AFSC/PAS 3-2-87

8763
Air Force Weapons Laboratory
Office of Public Affairs
Kirtland AFB, NM 87117-6008

FOREWORD

The authors are thankful to Lt. J. Crissey and Mr. Doug Craig of the Air Force Weapons Laboratory, and Mr. Pat Elliott of Maxwell Laboratory, Inc. for their support and encouragement. Thanks are also due to Mr. Stuart H. Sands of LuTech, Inc. for his assistance with some of the numerical computations.

CONTENTS

<u>Section</u>	<u>Page</u>
I. INTRODUCTION	3
II. INCREMENTAL MODEL OF TWO-PERFECT-CONDUCTOR TRANSMISSION LINE	6
III. APPROXIMATION OF A SECTION OF BURIED TRANSMISSION LINE BY CASCADED SECTIONS OF INCREMENTAL MODELS . .	13
IV. CHOICE OF CASCADED SECTION LENGTHS FOR LUMPED- ELEMENT APPROXIMATION	19
V. CONSIDERATIONS OF ALTERNATE CURRENT PATHS AT THE TERMINATION PORT.	22
VI. AN ILLUSTRATIVE EXAMPLE	24
VII. SUMMARY	45
REFERENCES	46

I. INTRODUCTION

There are various techniques to simulate the nuclear EMP, including in or near source regions as discussed in [1]. A nuclear EMP near the air-earth interface results in a large distributed electromagnetic source on the interface. Such an electromagnetic source produces an underground field that propagates very nearly perpendicular to the interface. In the context of simulating this underground field, past works [2 to 5] have addressed the problem of analyzing a buried transmission line formed by vertical "plates" of perfectly conducting material. (Actually such plates are constructed in practice as arrays of vertical rods in the ground).

Schematically, this simulation technique is shown in figure 1.1. In this geometry, we have the two vertical conductors in the shape of plates of width $2a$, separation $2b$ and length l , the constitutive parameters of the ground medium are denoted by conductivity σ , permittivity $\epsilon = \epsilon_0 \epsilon_r$ and permeability μ_0 . The above half space is air with zero conductivity, permittivity ϵ_0 and permeability μ_0 . A rectangular (x,y,z) coordinate system is used with the (x,y) plane as the air-ground interface. The x and y axes are respectively in the directions of the principal magnetic and electric fields and the electromagnetic field is propagating in the negative z direction. In an actual site, the "plates" are made up of practical grids of conducting rods.

There are some limitations to such a simulation technique. For example, the surface fields may be changing significantly over a certain distance, such as the mean free path of the gamma ray r_γ from an EMP. In the model, the horizontal dimensions $2a$ or $2b$, the ground skin depth δ should all be small compared to r_γ . The fringing fields near the top and bottom of the model also limit the model in these regions, unless one can compensate for such distortions, in some fashion.

The subject of this note is to investigate and design a suitable "load" at the end of the buried transmission line so that the electromagnetic field propagating downward into the ground is properly terminated.

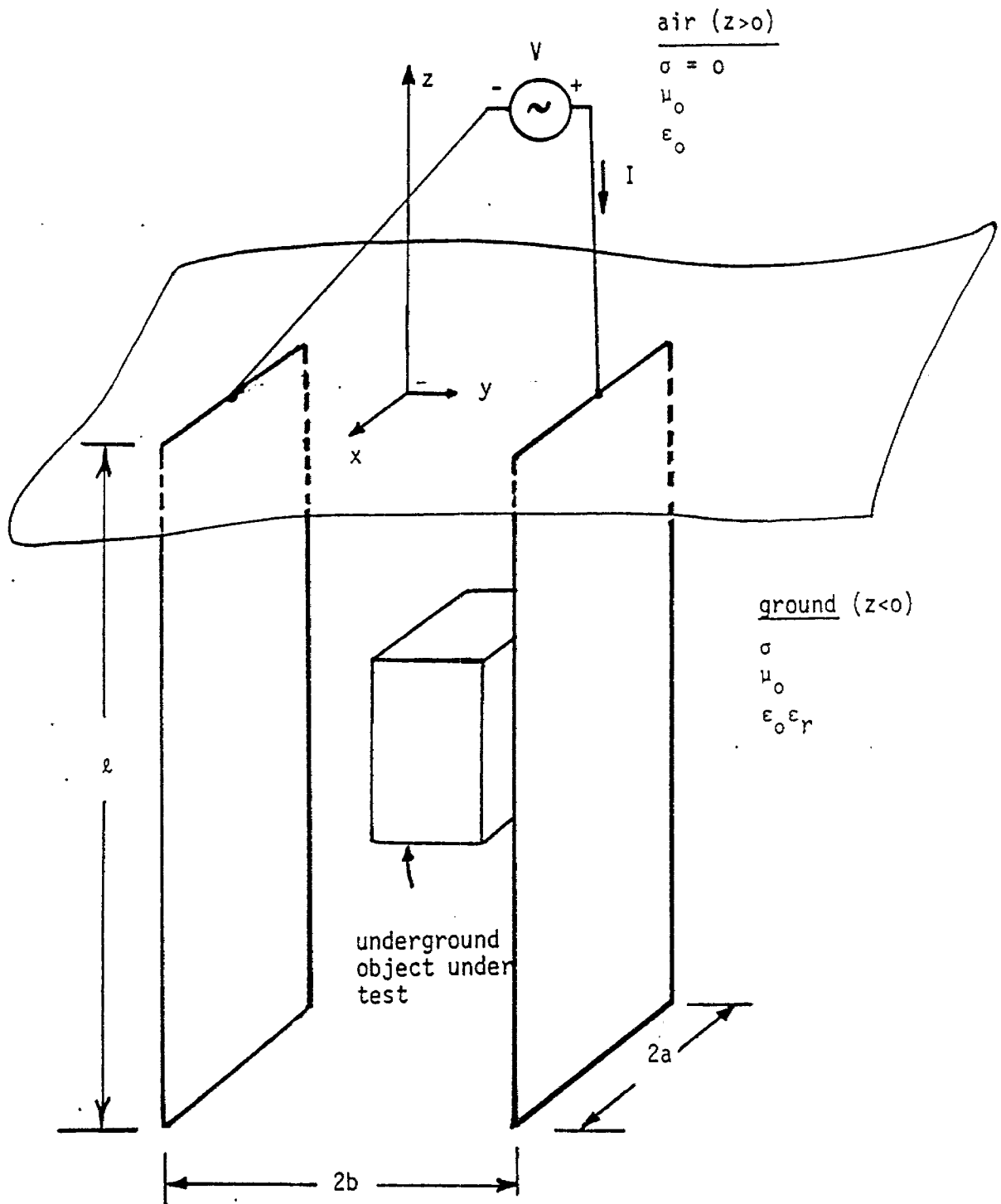


Figure 1.1 A buried transmission line formed by two vertical perfect conductors (rod arrays in practice).

While terminating a transmission line, one normally thinks of choosing the load impedance Z_L to be the same as the characteristic impedance $Z_C^{(TEM)}$ of the principal TEM mode of propagation, in order to obtain the condition of a matched load. This impedance is of course frequency dependent because of the ground medium, and it is known [2].

In developing the buried-transmission-line simulation technique it is useful to be able to replace all or a portion of the buried transmission line by some equivalent network which possesses the same impedance and/or transfer properties. For laboratory tests in which the buried-transmission-line properties must be combined with other equipment, such a network can be usefully employed.

One could think of replacing the very long transmission line of length ℓ by one of shorter length ℓ_0 (near the ground surface) and then divide the remaining length of $\ell_1 = (\ell - \ell_0)$ extending from $z = -\ell_0$ to $z = -\ell$ by sections. These individual sections are represented by their incremental lumped-element models, out of which a lumped-element network can be constructed to replace the remaining (lower) section of transmission line for $-\ell_0 > z > -\ell$.

In this introductory section, the need as well as an approach in constructing a lumped-element network as a replacement for all or part of the buried transmission line has been discussed. Section II reviews the incremental model of a two conductor transmission line, which is then applied in Section III to approximate sections of buried transmission line. Considerations of how one may divide the extended transmission line into sections for lumped element equivalents are discussed in Section IV. Section V discusses the alternate current paths at $z = -\ell_0$ for connecting the lumped element network, followed by an illustrative example network in Section VI. The note ends with summarizing remarks in Section VII followed by a list of references.

II. INCREMENTAL MODEL OF TWO-PERFECT- CONDUCTOR TRANSMISSION LINE

The buried transmission line of figure 1.1, formed by the vertical "plates" of perfectly conducting material may be represented schematically by a two conductor transmission line as indicated in figure 2.1. The equations governing the voltage and current propagation on such a transmission line are given by [6]

$$\frac{d}{dz} \tilde{I}(z,s) = -\tilde{Y}'(s) \tilde{V}(z,s) + \tilde{I}^{(s)'}(z,s)$$

$$\frac{d}{dz} \tilde{V}(z,s) = -\tilde{Z}'(s) \tilde{I}(z,s) + \tilde{V}^{(s)'}(z,s)$$

z = position along the transmission line

$s \equiv$ complex frequency = $\Omega + j\omega$

$\tilde{I}(z,s)$ = current at location z

$\tilde{V}(z,s)$ = voltage at location z (2.1)

$\tilde{Y}'(s)$ = per-unit-length shunt admittance

$\tilde{Z}'(s)$ = per-unit length series impedance

$\tilde{I}^{(s)'}(z,s)$ = per-unit-length shunt current source

$\tilde{V}^{(s)'}(z,s)$ = per-unit-length series voltage source

The distributed sources along the transmission line represented by $\tilde{I}^{(s)'}(z,s)$ and $\tilde{V}^{(s)'}(z,s)$ are included for completeness in the per-unit-length model shown in figure 2.2. They are not always present, and an example situation when the distributed sources are required is when there is an electromagnetic wave incident on the transmission line. In the per-unit-length model, the series impedance $\tilde{Z}'(s)$ and shunt admittance $\tilde{Y}'(s)$ per unit length are also indicated. So, in effect the long transmission line is made up of an appropriate number of cascaded sections of per-unit-length models.

There are a few different ways of solving (2.1), one of which is to write a second order differential equation each for the voltage and current alone and solve for these quantities. Since our present interest is in the

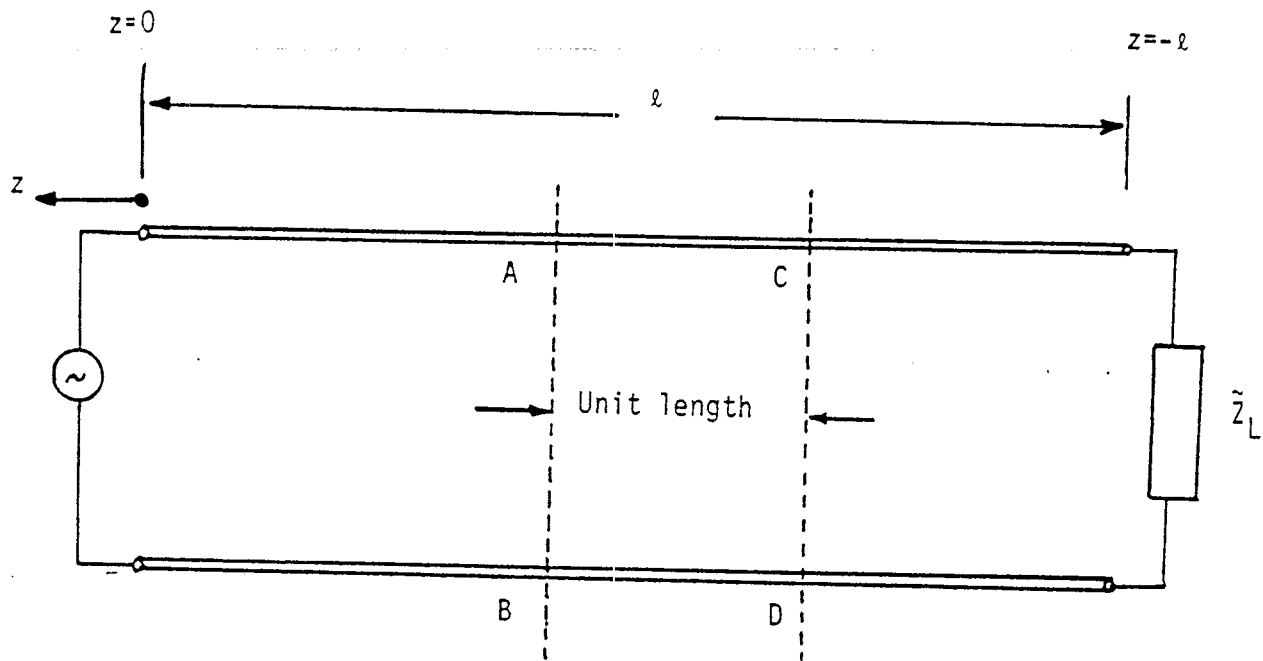


Figure 2.1 Two-perfect conductor transmission line.

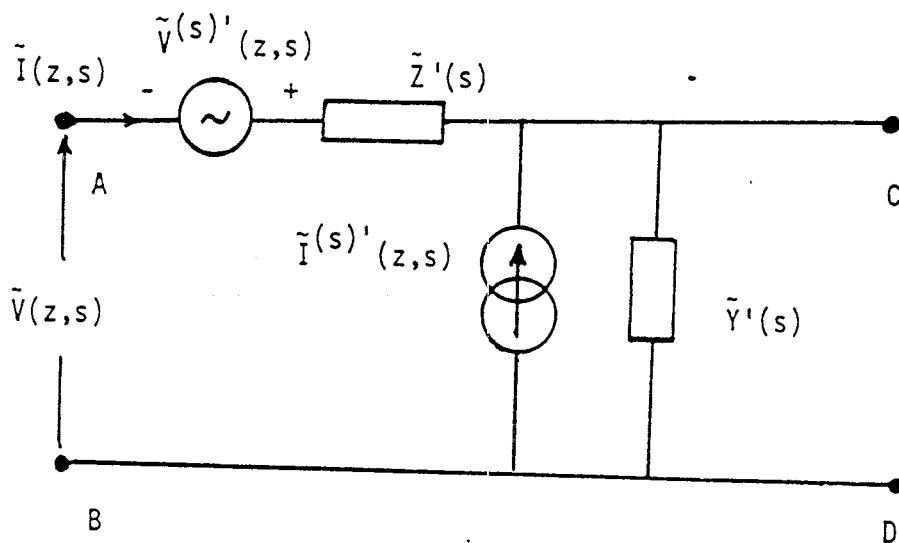


Figure 2.2 The per-unit-length model of a two conductor transmission line.

per-unit-length model, the solution of (2.1) is not reviewed here. It is also noted that the per-unit-length model is easily converted to an incremental length model applicable for a length dz of the transmission line. In the absence of any distributed sources along the transmission line, as is applicable in the problem at hand, the per-unit-length model of figure 2.2 is somewhat simplified and is shown in figure 2.3. It is observed that the series impedance $\tilde{Z}'(s)$ per unit length is made up of a series resistance R' and inductance L' per unit length. Similarly the shunt admittance $\tilde{Y}'(s)$ per unit length consists of a conductance G' and capacitance C' per unit length. The incremental-length model is derivable from the per-unit-length model as shown in figure 2.4.

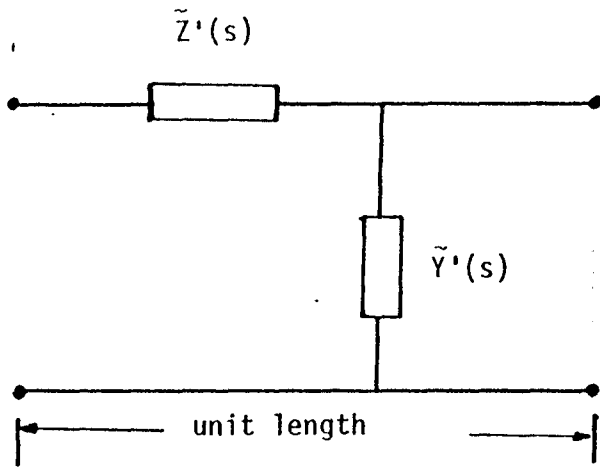
It is also noted that certain approximations to these models may be valid under certain conditions. For example, if this transmission line were made up of perfect conductors immersed in a uniform lossless medium, R' and G' vanish, resulting in a line with per-unit-length inductance and capacitance only.

In the present example of a perfectly conducting buried transmission line, R' may be neglected. In addition C' may be neglected at frequencies where the conduction current in the medium ($\sigma\vec{E}$) dominates over the displacement current ($\dot{\vec{D}}$). On the imaginary axis of the complex frequency domain, this implies $\sigma \gg \omega\epsilon$. In general, with assumed perfect conductors, we have

$$\begin{aligned}\tilde{Z}'(s) &= s\mu f_g \\ \tilde{Y}'(s) &= (\sigma + s\epsilon)/f_g\end{aligned}\tag{2.2}$$

where f_g is the geometrical factor for the transmission line, which relates the impedance of an infinitely long transmission line \tilde{Z}_{L_∞} with the wave impedance \tilde{Z} according as

$$\tilde{Z}_{L_\infty} = \tilde{Z}_c^{(TEM)} = f_g \tilde{Z}(s)\tag{2.3}$$



≡

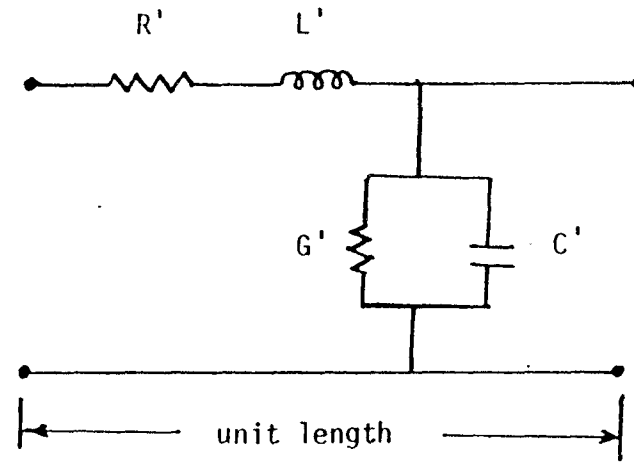
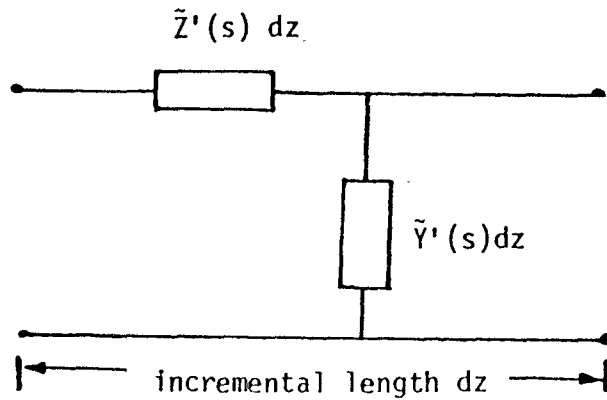


Figure 2.3 Per-unit-length model with no distributed sources.

6



≡

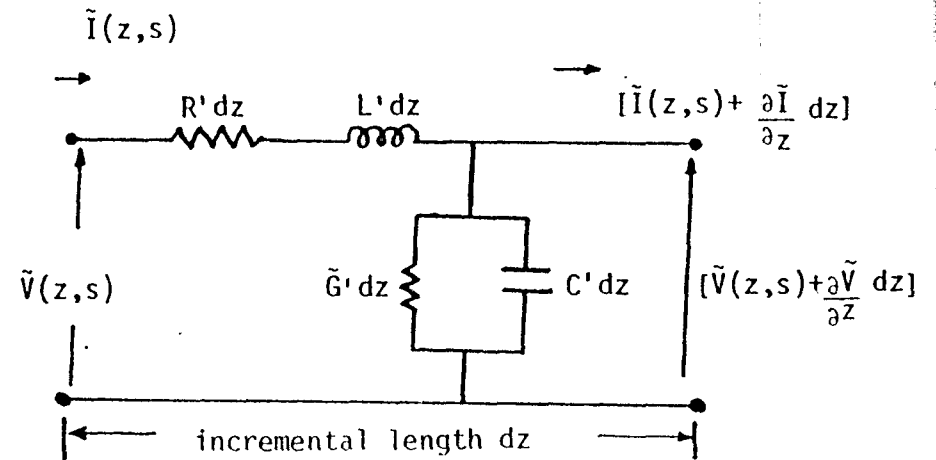


Figure 2.4 Differential length (\$dz\$) models with no distributed sources.

The wave impedance is given by

$$\tilde{Z}(s) = \left(\frac{s\mu}{\sigma + s\epsilon} \right)^{1/2} \quad (2.4)$$

certain simplifications are possible under the low frequency assumption of $\sigma \gg |s\epsilon|$, resulting in

$$\begin{aligned} R' &= 0 && \text{(perfect conductor assumption)} \\ L' &= \mu_0 f_g && \text{(for assumed nonmagnetic medium } \mu_r = 1) \\ G' &= \sigma / f_g \\ C' &= \text{negligible} \end{aligned} \quad (2.5)$$

The characteristic impedance \tilde{Z}_c under these assumptions is then given by

$$\tilde{Z}_c(s) = \tilde{Z}_{L_\infty}(s) = f_g \sqrt{\frac{s\mu_0}{\sigma}} = \sqrt{\frac{sL'}{G'}} \quad (2.6)$$

The approximate i.e., low-frequency and perfect-conductor assumptions being valid, the incremental model is then further simplified as shown in figure 2.5. This model is derivable from the transmission line equations as follows.

The transmission line equations in time and frequency domains become

$$\frac{dI(z,t)}{dz} = -G' V(z,t) \quad (2.7)$$

$$\frac{dV(z,t)}{dz} = -L' \frac{dI(z,t)}{dt}$$

$$\frac{d\tilde{I}(z,s)}{dz} = -G' \tilde{V}(z,s) \quad (2.8)$$

$$\frac{d\tilde{V}(z,s)}{dz} = -sL' \tilde{I}(z,s)$$

Equation (2.8) may also be written as a difference equation and applied to obtain the incremental models of figures 2.5 and 2.6.

$$\tilde{I}(z+dz,s) = \tilde{I}(z,s) - (G'dz) \tilde{V}(z,s) \quad (2.9)$$

$$\tilde{V}(z+dz,s) = \tilde{V}(z,s) - s(L'dz) \tilde{I}(z,s)$$

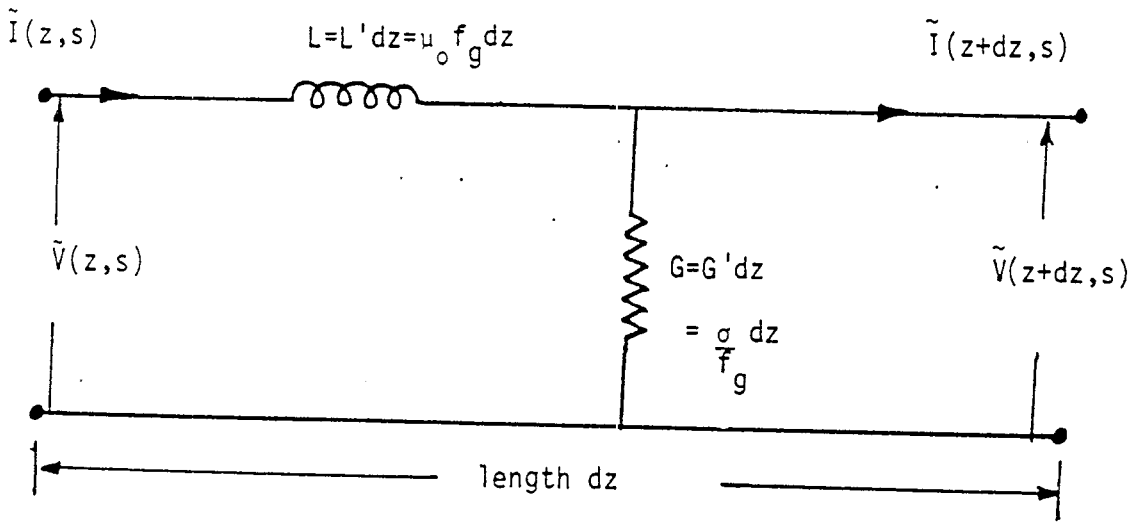


Figure 2.5 Low frequency, incremental-length model of the buried transmission line made of perfect conductors.

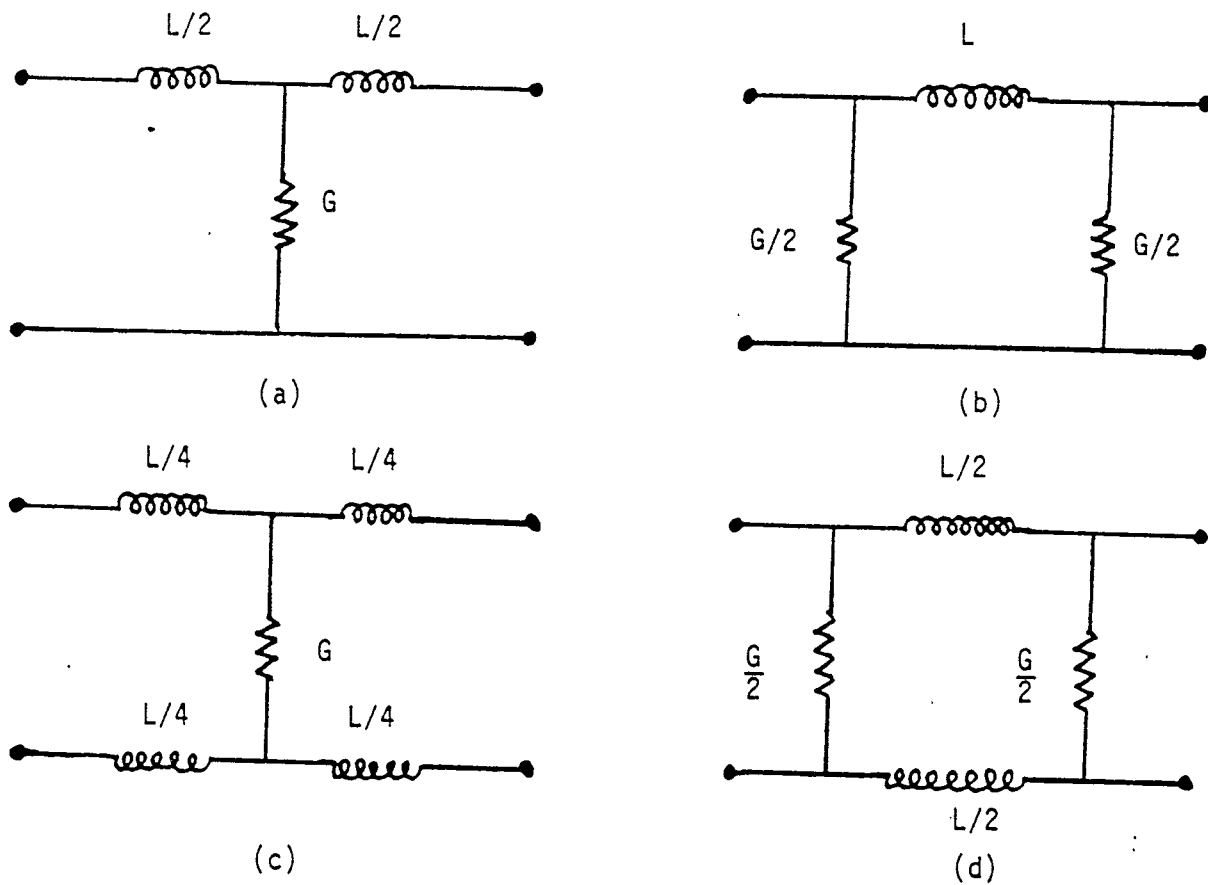


Figure 2.6 Other equivalent forms of the model in figure 2.5.

The above equation is represented by its lumped element model in figure 2.5.

Other equivalent forms of the circuit of figure 2.5 are shown in figure 2.6. The incremental model outlined above is applied to approximate a portion of the buried transmission line of figure 1.1, in the following section.

III. APPROXIMATION OF A SECTION OF BURIED TRANSMISSION LINE BY CASCADED SECTIONS OF INCREMENTAL MODELS

The incremental model of a buried transmission line discussed in the preceding section is now applied to a buried transmission line of length ℓ indicated on the left of figure 3.1. Such a long line in the earth medium can be replaced by a shorter line of length ℓ_0 and a suitable frequency dependent network connected across the bottom end as indicated on the right of figure 3.1. The purpose of the network then is to "simulate" the impedance \tilde{Z}_L looking down at the cross section AB. In other words the input impedance \tilde{Z}_{in} of the network is the same as the open-circuit impedance of a buried section of transmission line of length $\ell_1 = (\ell - \ell_0)$. This theoretical impedance \tilde{Z}_{L_1} is given by [2],

$$\tilde{Z}_{L_1}(s) = \tilde{Z}_{L_\infty}(s) \left[\frac{1 + e^{-2\gamma\ell_1}}{1 - e^{-2\gamma\ell_1}} \right] \quad (3.1)$$

where

$$\begin{aligned} \gamma &\equiv \text{complex propagation number in the earth or soil medium} \\ &= [s\mu_0(\sigma + s\epsilon)]^{1/2} \\ &\approx \sqrt{s\mu_0\sigma} \quad \text{at low frequencies } (\sigma \gg |s\epsilon|) \end{aligned} \quad (3.2)$$

and $\tilde{Z}_{L_\infty}(s)$ is expressed in (2.3) and (2.4). So, collecting all the results, (3.1) may be written as

$$\begin{aligned} \tilde{Z}_{L_1}(s) &= f_g \left(\frac{s\mu_0}{\sigma + s\epsilon} \right)^{1/2} \left[\frac{1 + e^{-2\gamma\ell_1}}{1 - e^{-2\gamma\ell_1}} \right] \\ &= f_g \left(\frac{s\mu_0}{\sigma + s\epsilon} \right)^{1/2} \coth(\ell_1 \sqrt{s\mu_0(\sigma + s\epsilon)}) \end{aligned} \quad (3.3)$$

At low frequencies ($\sigma \gg |s\epsilon|$), and if the line is electrically small i.e. $|\ell_1 \sqrt{s\mu_0\sigma}| \ll 1$, (3.3) simplifies to

$$\tilde{Z}_{L_1}(s) \approx f_g \left[\frac{1}{\ell_1\sigma} + \frac{s\mu_0\ell_1}{3} \right] \quad (3.4)$$

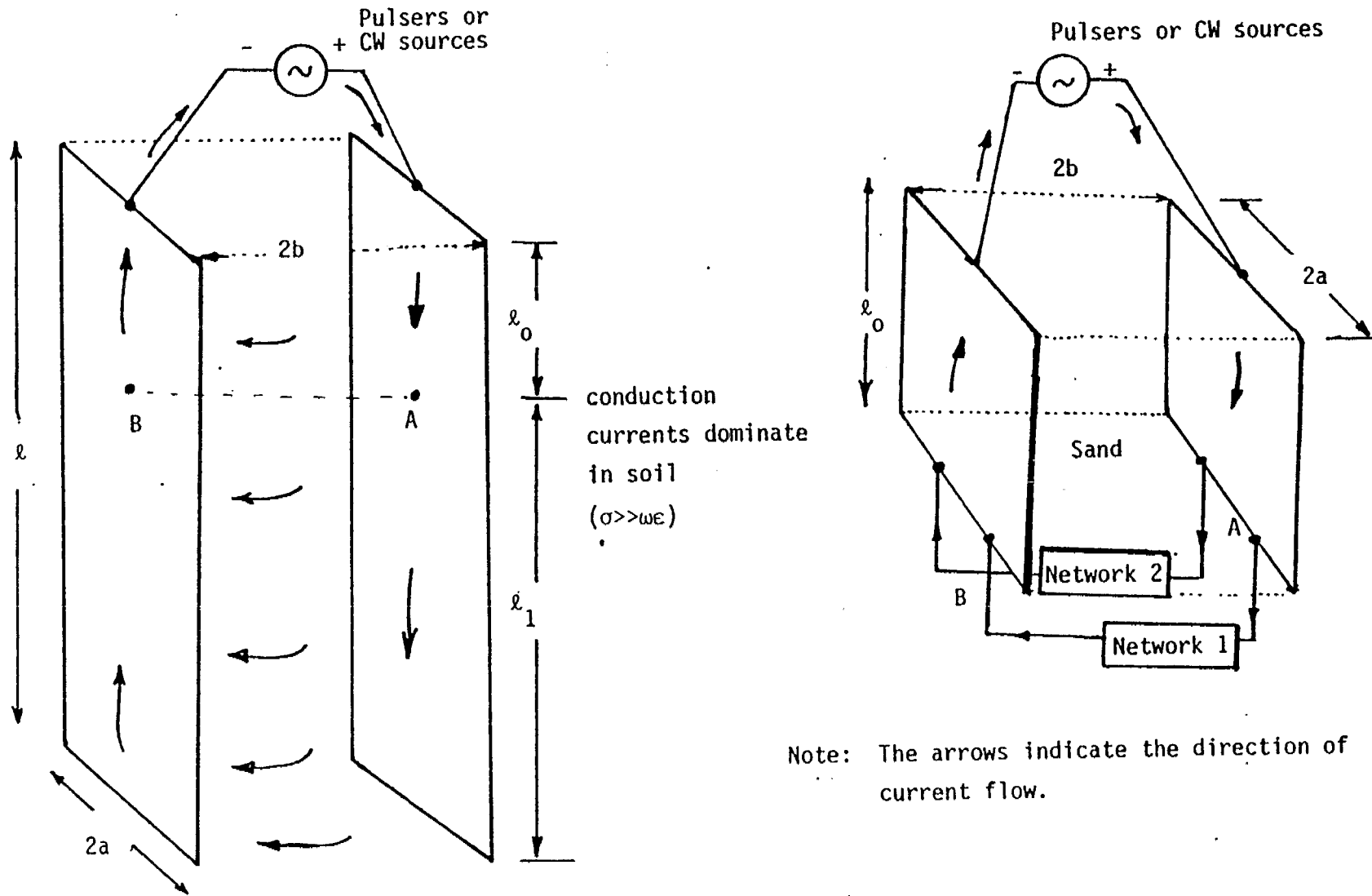


Figure 3.1 Simulation of a long buried transmission line by one that is shorter and terminated by a suitable network(s) connected in parallel across the bottom end.

The goal of the lumped element network is then to simulate the above impedance $\tilde{Z}_{L_1}(s)$. The network is derived by dividing the ℓ_1 of the transmission line ($= \ell - \ell_0$) by a certain number of sections N_s , writing a lumped element incremental model for each section and combining the shunt elements to arrive at the final network. This procedure is described below.

Consider the two-perfect-conductor transmission line of length ℓ_1 as shown at the top of figure 3.2. With reference to the z coordinate of figure 1.1, this line extends from $z = -\ell_0$ to $z = -\ell$ and, is of length $\ell_1 = (\ell - \ell_0)$. This line is then divided into N_s number of sections as indicated in the mid-section of figure 3.2. These sections or portions of the transmission line are designated by $P_1, P_2 \dots P_{N_s}$. Each of these sections is then represented by its incremental model as shown at the bottom of figure 3.2. The symmetric incremental model of figure 2.6(d) is used in this illustration. Note that the series and shunt elements of each section are simply given by the per-unit-length parameters multiplied by the section length, according as

$$\left. \begin{aligned} \tilde{Z}_n(s) &= \tilde{Z}'(s) \Delta\ell_n \\ \tilde{Y}_n(s) &= \tilde{Y}'(s) \Delta\ell_n \end{aligned} \right\} \quad \text{for } n = 1, 2 \dots N_s \quad (3.5)$$

where $\Delta\ell_n$ is the length of the n th section given by

$$\Delta\ell_n = |z_{n+1} - z_n| \quad \text{for } n = 1, 2 \dots N_s \quad (3.6)$$

and the line constants or the per-unit-length parameters $\tilde{Z}'(s)$ and $\tilde{Y}'(s)$ are given by (2.2) under a perfect-conductor approximation.

In addition to the perfect conductor approximation ($R' = 0$), if we are concerned with low frequencies, i.e. $\sigma \gg |s\epsilon|$, and if each section is electrically small, i.e. $|\Delta\ell_n \sqrt{s\mu_0 \sigma}| \ll 1$, then the lumped element network of figure 3.2 simplifies to what is shown in figure 3.3. The simplification results from neglecting the shunt capacitances

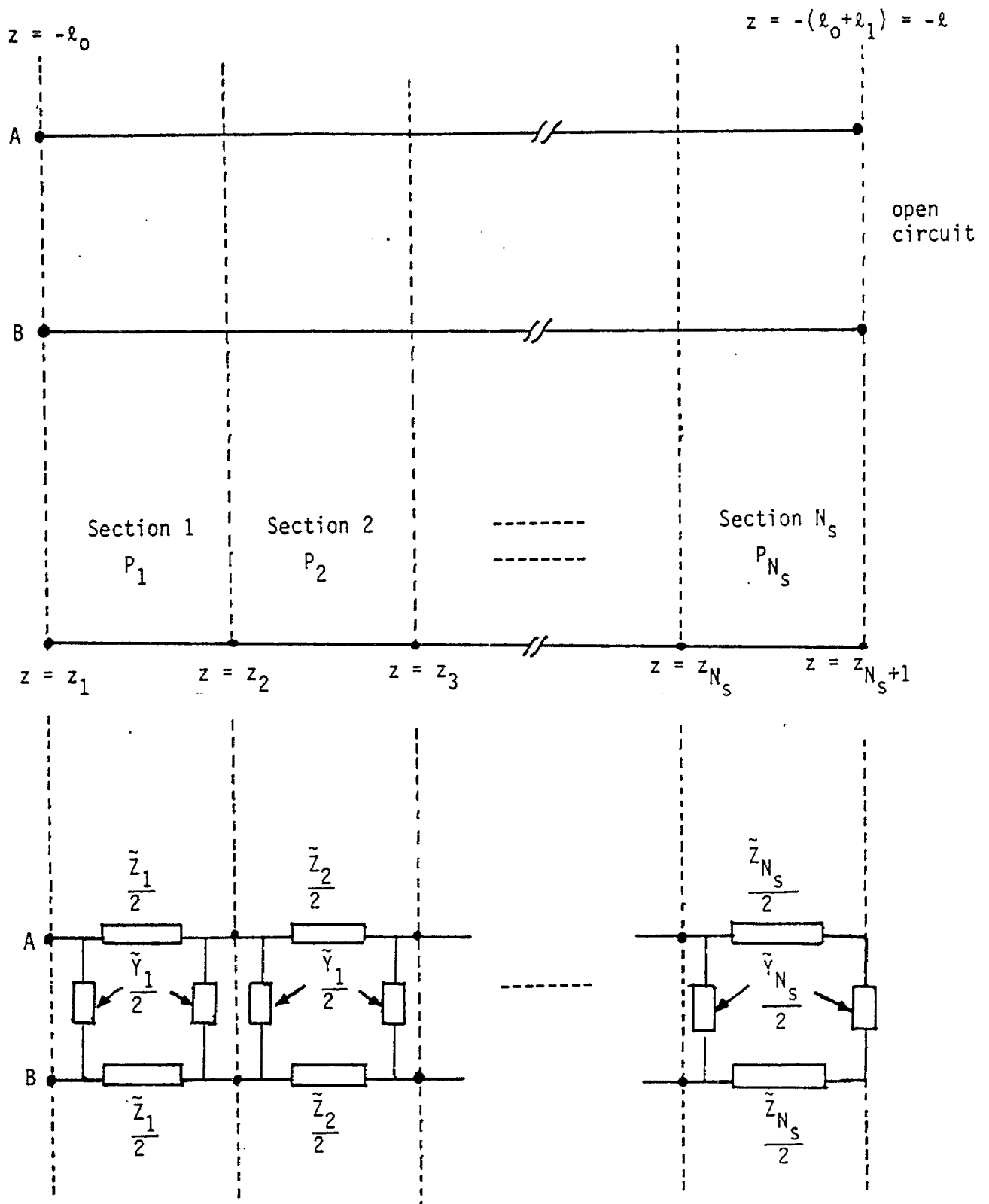


Figure 3.2. Development of the network by cascading the low frequency incremental models.

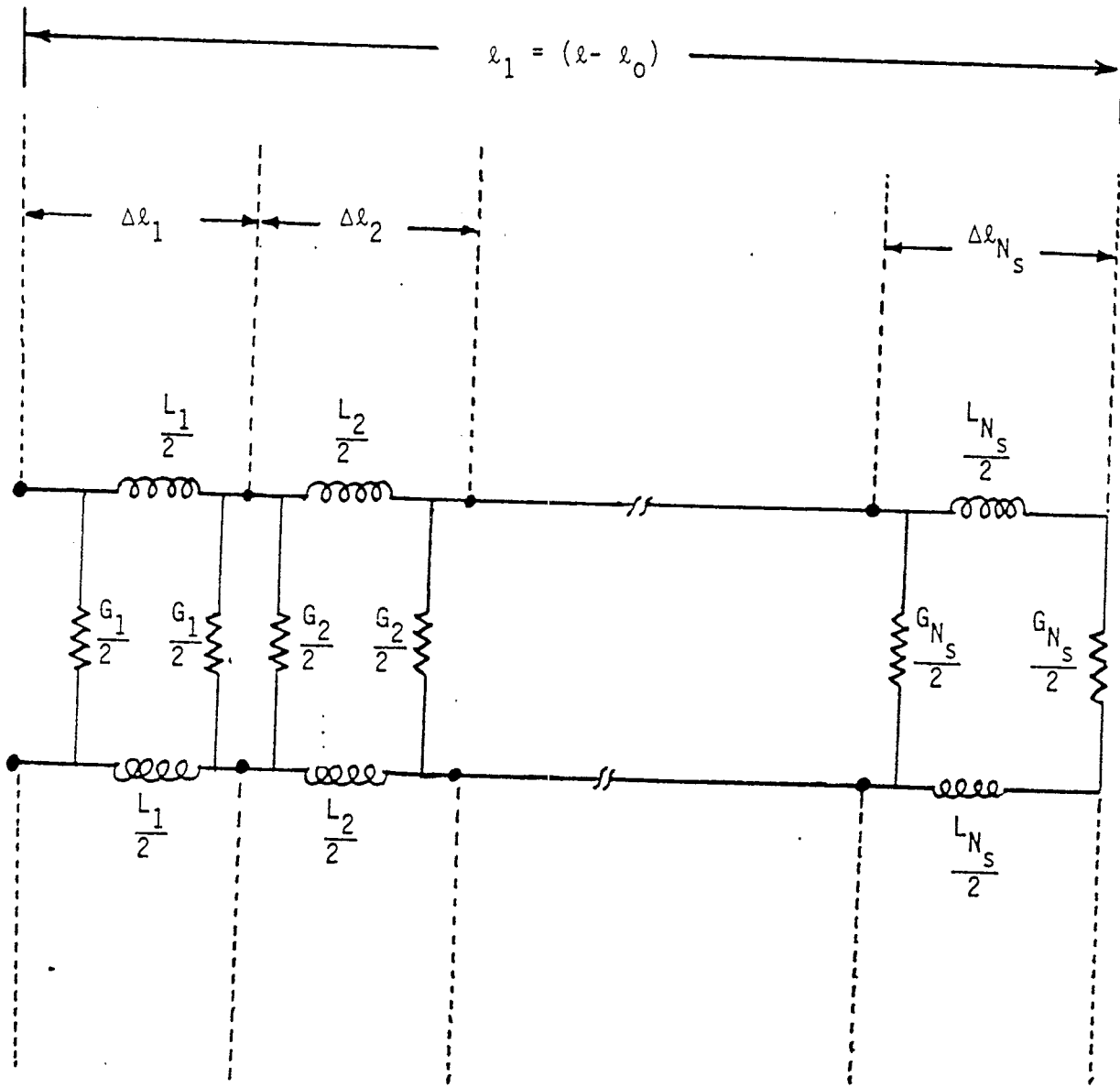


Figure 3.3. Approximate lumped element network at low frequencies, for a buried transmission line of length l_1 .

from the incremental models, in comparison with the shunt conductances. The elements of this approximate network are then given by

$$\begin{aligned}
 L_n &= L' \Delta \ell_n \\
 &= \mu_0 f_g \Delta \ell_n \\
 &= \mu_0 f_g (z_{n+1} - z_n) \quad \text{for } n = 1, 2 \dots N_s \quad (3.7)
 \end{aligned}$$

and

$$\begin{aligned}
 G_n &= G' \Delta \ell_n \\
 &= \frac{\sigma}{f_g} \Delta \ell_n \\
 &= \frac{\sigma}{f_g} (z_{n+1} - z_n) \quad \text{for } n = 1, 2 \dots N_s \quad (3.8)
 \end{aligned}$$

The above derivation formally completes the procedure of arriving at the lumped element network representation for a section of open-circuited and buried transmission line. However, there are some practical aspects of such networks that have not been addressed yet. For example, the choice of section lengths $\Delta \ell_n$ which are not all necessarily the same and the actual connection of the network(s) at the bottom of the shorter transmission line of length ℓ_0 , are important design and fabrication related issues. These two topics form the subjects for the following two sections.

IV. CHOICE OF CASCADED SECTION LENGTHS FOR LUMPED-ELEMENT APPROXIMATION

In this section, we address the question of choosing Δl_n for $n = 1, 2, \dots, N_s$. These are the lengths of the individual sections into which the buried transmission line is divided for representation via the incremental model, and realization by corresponding lumped networks.

Note that the fields diffuse into the soil medium according as $e^{\gamma z}$. Using (3.2) we have,

$$\begin{aligned} e^{\gamma z} &\equiv \exp\left(z \sqrt{s\mu_0(\sigma + s\epsilon)}\right) \\ &\approx \exp(z \sqrt{s\mu_0\sigma}) \quad (\text{at low frequencies}) \end{aligned} \quad (4.1)$$

setting $s = j\omega$,

$$\begin{aligned} e^{\gamma z} &\approx \exp\left\{z(1+j)\sqrt{\frac{\omega\mu_0\sigma}{2}}\right\} \\ &= \exp\left\{(1+j)\frac{z}{\delta}\right\} \end{aligned} \quad (4.2)$$

where δ is the skin depth defined by

$$\delta = \sqrt{\frac{2}{\omega\mu_0\sigma}} \quad (4.3)$$

The above expression leads to

$$e^{\gamma z} \approx e^{(1+j)z/\delta} \quad (4.4)$$

or

$$|e^{\gamma z}| \approx e^{z/\delta} \quad (4.5)$$

where z is negative. Therefore, for a given radian frequency ω , we are only concerned with distances $|z| < \delta$ and the medium beyond $|z| > \delta$ has negligible influence on the input impedance. In addition, once the wave has propagated one skin depth distance, the reflected signal back at the air-soil interface is e^{-2} (=13.5 percent) or less. The implication here is that only sections within one skin depth need to be electrically small, i.e.

$$\left(\frac{\Delta \ell}{\delta}\right) \ll 1 \quad (4.6)$$

But, we necessarily have $(\Delta \ell_n < z_{n+1})$, and hence if $(z_{n+1} < \delta)$ then $(\Delta \ell_n < \delta)$. For our present purposes let us choose $\Delta \ell_n$ to be of the order of $(z_{n+1}/2)$. Furthermore for the initial section, i.e., $0 > z > -\ell_0$, let us use the actual conducting medium (e.g., soil) and represent the remaining portion of the buried transmission line extending from $z = -\ell_0$ to $z = -\ell$ by lumped networks. This choice then "hides" the first network section, disallowing unacceptably high frequencies from reaching this first network section. This choice also ensures that all network sections will meet the requirements of a section while substituting for electrically small portions of buried transmission line at relevant frequencies. In order to illustrate the above choice, let us consider an example of a buried transmission line of total length $\ell = 100\text{m}$. We choose to replace it by a buried line of length $\ell_0 = 2\text{m}$ and the remainder of $\ell_1 = 98\text{m}$ by a lumped element network with the appropriate impedance and/or transfer properties. Also, a choice of the number of sections $N_s = 5$ is made according as

$$\begin{array}{ll}
 -z_1 = \ell_0 = 2\text{m} & \Delta \ell_1 = 4\text{m} \\
 -z_2 = 6\text{m} & \Delta \ell_2 = 6\text{m} \\
 -z_3 = 12\text{m} & \Delta \ell_3 = 13\text{m} \\
 -z_4 = 25\text{m} & \Delta \ell_4 = 25\text{m} \\
 -z_5 = 50\text{m} & \Delta \ell_5 = 50\text{m} \\
 -z_6 = 100\text{m} &
 \end{array}
 \quad \Rightarrow \quad (4.7)$$

Note that $\Delta\ell_n \approx |z_{n+1}/2|$ in the above scheme. As one goes deeper into the soil, corresponding to the end sections, increasingly lower frequencies are able to penetrate the medium so that the skin depth is larger and the sections can get successively longer and still meet the requirement of being electrically small. It is also observed that

$$\sum_{n=1}^{N_s=5} \Delta\ell_n = \ell_1 = (\ell - \ell_0) = 98\text{m (for this example)} \quad (4.8)$$

The above choice has been implemented in practice and the results are encouraging, as reported in a later section of this note. Prior to the discussion of this illustrative example, we have addressed the question of the actual connection of the network(s) to the shorter section ℓ_0 of the transmission line in the following section.

V. CONSIDERATIONS OF ALTERNATE CURRENT PATHS AT THE TERMINATION PORT

Referring to figure 3.1, it is recalled that the buried transmission line extending from $z = -\ell_0$ to $z = -\ell$ is being replaced by the lumped network. This implies that the current carried by the network from one vertical conductor to the other must approximate the total distributed current in the soil medium contained in the region $z = -\ell_0$ to $z = -\ell$. Proper input impedance of the network assures that this requirement on the total current is met under the assumed conditions. In practice, the soil medium is truncated at $z = -\ell_0$ by employing perhaps a dielectric sand box and the network is hooked on at the bottom on the outside of such a sand box.

However, in addition to the requirement on the total current through the network, the network should carry its current in such a way that the magnetic field in the region $z = 0$ to $z = -\ell_0$ is approximately the same as if the buried transmission line extended all the way to $z = -\ell$.

In attempting to meet the above requirements, two possible choices of connecting the network are indicated in figures 5.1 and 5.2. Figure 5.1 shows one network which is connected at the mid point along the width of the vertical "plates". Figure 5.2 shows two networks connected along the width at two points separated by one-third the plate width. Clearly, since the current path in the actual soil medium ($-\ell_0 > z > -\ell$) is distributed, having two networks is better than one. However the connection points of the two networks is best optimized experimentally by monitoring the magnetic field in the region extending from $z = 0$ to $z = -\ell_0$. The illustrative example of Section IV uses two networks as indicated in figure 5.2. It is also noted that when one uses two identical networks in parallel, each is designed to have twice the required impedance so that their parallel combination provides the desired impedance.

In the following section, an illustrative design example is considered in detail.

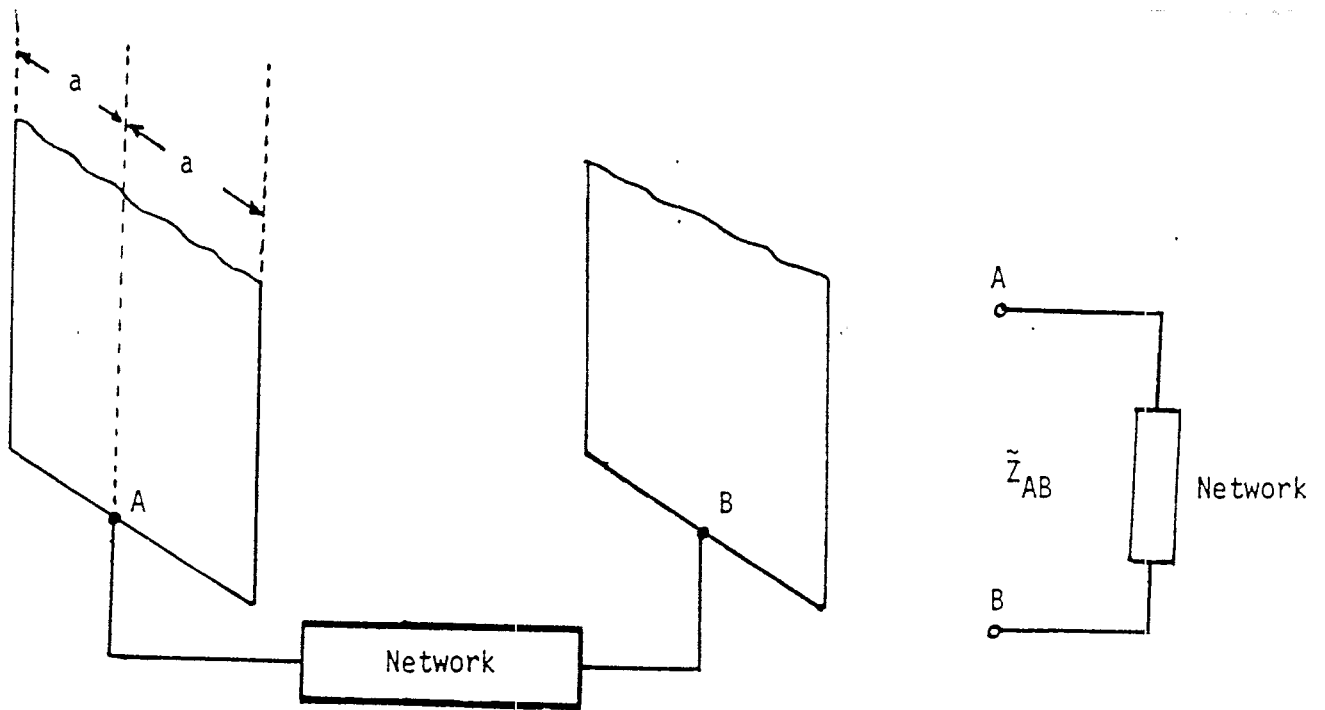


Figure 5.1. Network connection at the midpoint of the bottom end of plates.

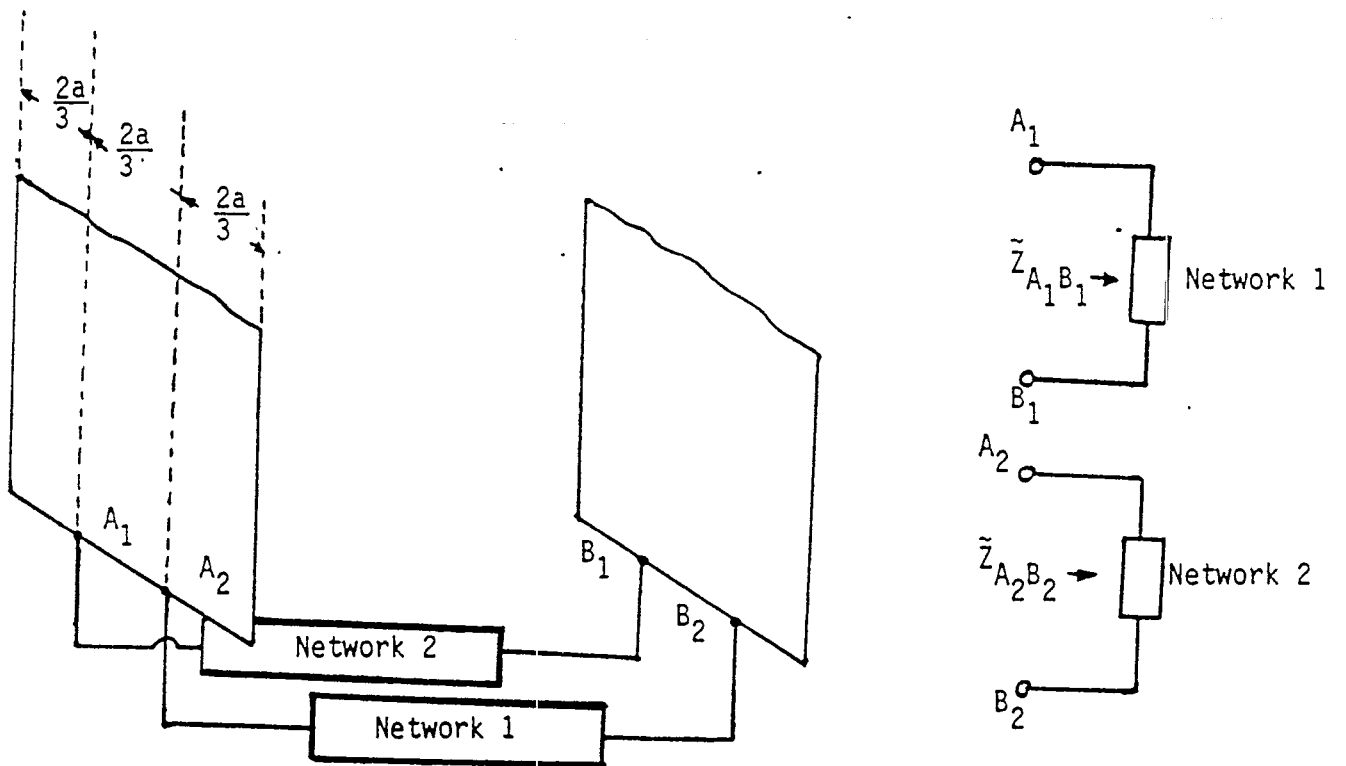


Figure 5.2. 2 Networks in parallel connected at terminals A_1B_1 and A_2B_2 which are a third of the plate width away from the edges.

Note the network impedance relationships

$$\tilde{Z}_{A_1B_1} = \tilde{Z}_{A_2B_2} = 2\tilde{Z}_{AB}$$

VI. AN ILLUSTRATIVE EXAMPLE

Consider a buried transmission line as in figure 1.1 with the following parameters

$$\begin{aligned}
 \ell &= 100\text{m} \\
 2b &= 4\text{m} \\
 2a &= 4\text{m} \\
 \mu &= \mu_0 = 4\pi \times 10^{-7} \text{ H/m} \\
 \sigma &= 10^{-2} \text{ S/m} \\
 \epsilon &= \epsilon_0 \epsilon_r \\
 \epsilon_0 &\approx 10^{-9}/(36\pi) \text{ F/m} ; \quad \epsilon_r = 10 \\
 f_g &= 0.4764
 \end{aligned} \tag{6.1}$$

Given the above numerical values, we first evaluate and plot the quantity $[\sigma/(\omega\epsilon)]$ and the skin depth δ as a function of frequency to determine the range of validity of the low-frequency approximation. The skin depth δ is given by

$$\delta = \sqrt{\frac{2}{\omega\mu_0\sigma}} \tag{6.2}$$

and it is independent of the dielectric constant ϵ_r . These two quantities are shown plotted in figures 6.1 and 6.2. The plot of figure 6.1 indicates that $\sigma > \omega\epsilon$ by an order of magnitude up to about 2 MHz. The skin depth is plotted for completeness, and incidentally to verify that the various sections meet the criterion of electrical smallness or equivalently $\Delta\ell_n < \delta$ at relevant frequencies.

The indication from figure 6.1 is that if one designs a network, good agreement may be expected between the impedance $\tilde{Z}_{L1}(s)$ of the open circuited transmission line and the impedance $\tilde{Z}_{LN}(s)$ of the network(s) both in magnitude and phase up to at least 1 MHz, after setting $s = j\omega = j 2\pi f$. Now, we may proceed to design the network(s) as follows. We have

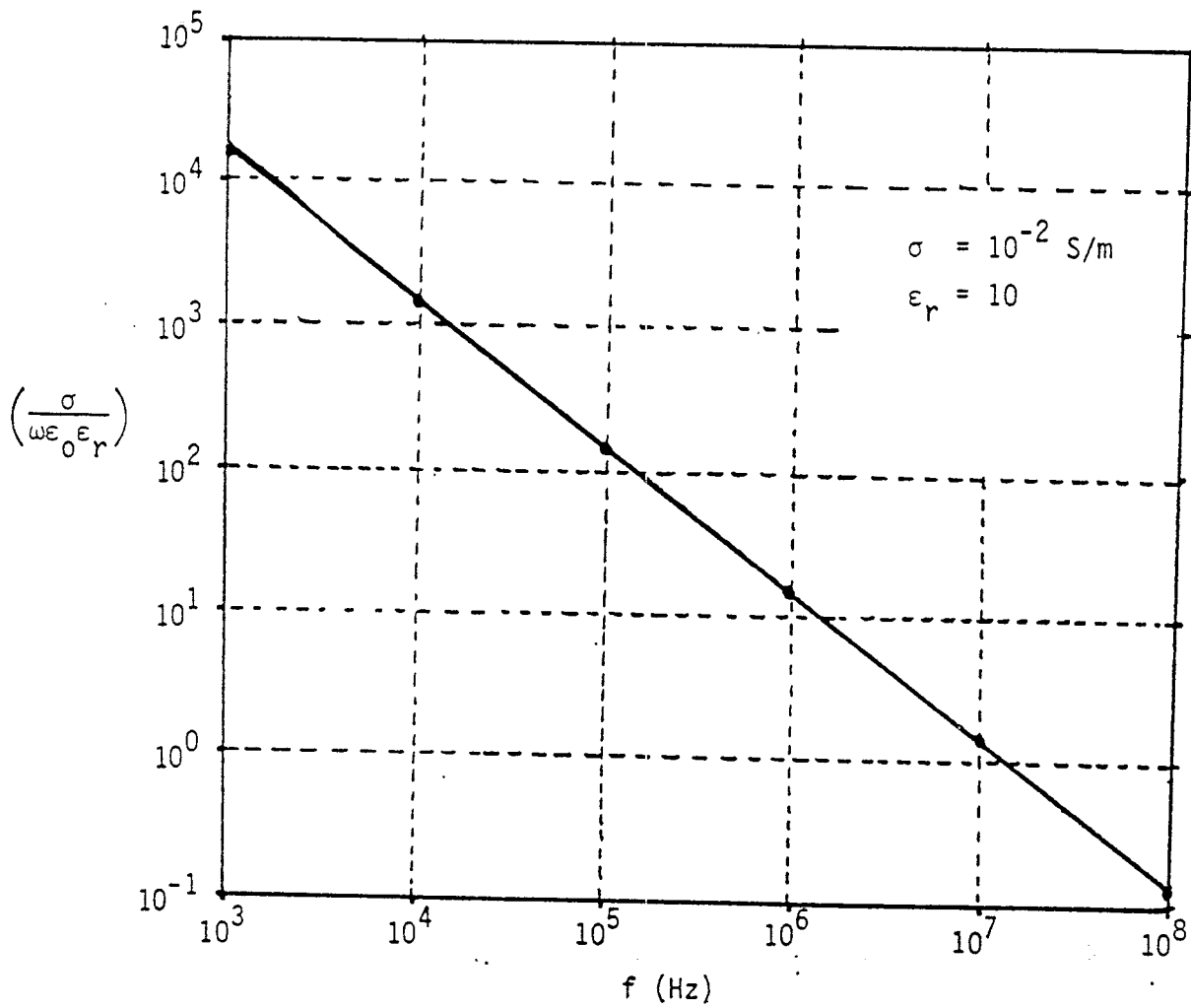


Figure 6.1. The loss tangent or the ratio of conduction to displacement currents in soil as a function of frequency.

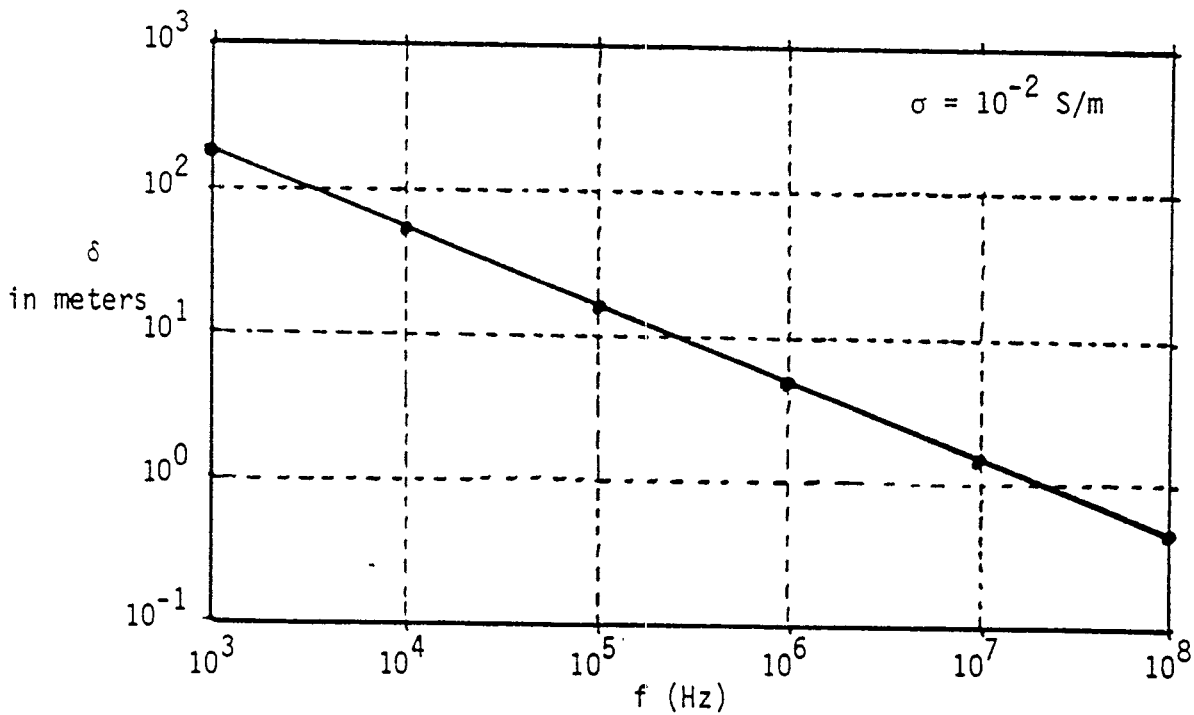


Figure 6.2. The skin depth δ of the soil medium as a function of frequency.

$$L' = \mu_0 f_g = 0.598 \text{ H/m} \quad (6.3)$$

$$G' = \frac{\sigma}{f_g} = 20.990 \text{ S/m}$$

As indicated earlier, let us also choose to represent the 100m line by a 2m long line of the same width and separation, while the remaining 98m of the buried line is represented by the network(s). We also make the following choice of sections as in (4.7),

$$\begin{array}{ll} -z_1 = \ell_0 = 2\text{m} & \Delta\ell_1 = 4\text{m} \\ -z_2 = 6\text{m} & \Delta\ell_2 = 6\text{m} \\ -z_3 = 12\text{m} & \Delta\ell_3 = 13\text{m} \\ -z_4 = 25\text{m} & \Delta\ell_4 = 25\text{m} \\ -z_5 = 50\text{m} & \Delta\ell_5 = 50\text{m} \\ -z_6 = 100\text{m} & \end{array} \quad (6.4)$$

Using (3.7) and (3.8) we get

$$\begin{array}{ll} L_1 = 2.39 \text{ } \mu\text{H} & G_1 = 0.084 \text{ S} \\ L_2 = 3.58 \text{ } \mu\text{H} & G_2 = 0.126 \text{ S} \\ L_3 = 7.77 \text{ } \mu\text{H} & G_3 = 0.273 \text{ S} \\ L_4 = 14.95 \text{ } \mu\text{H} & G_4 = 0.525 \text{ S} \\ L_5 = 29.9 \text{ } \mu\text{H} & G_5 = 1.050 \text{ S} \end{array} \quad (6.5)$$

The initial network consisting of the cascading of the five sections is shown in the top section of figure 6.3. It is seen that the adjacent shunt conductances can be combined resulting in the network shown in the mid section of figure 6.2. The bottom figure in figure 6.3 merely indicates the shunt elements as the more familiar resistors by inverting the conductance values.

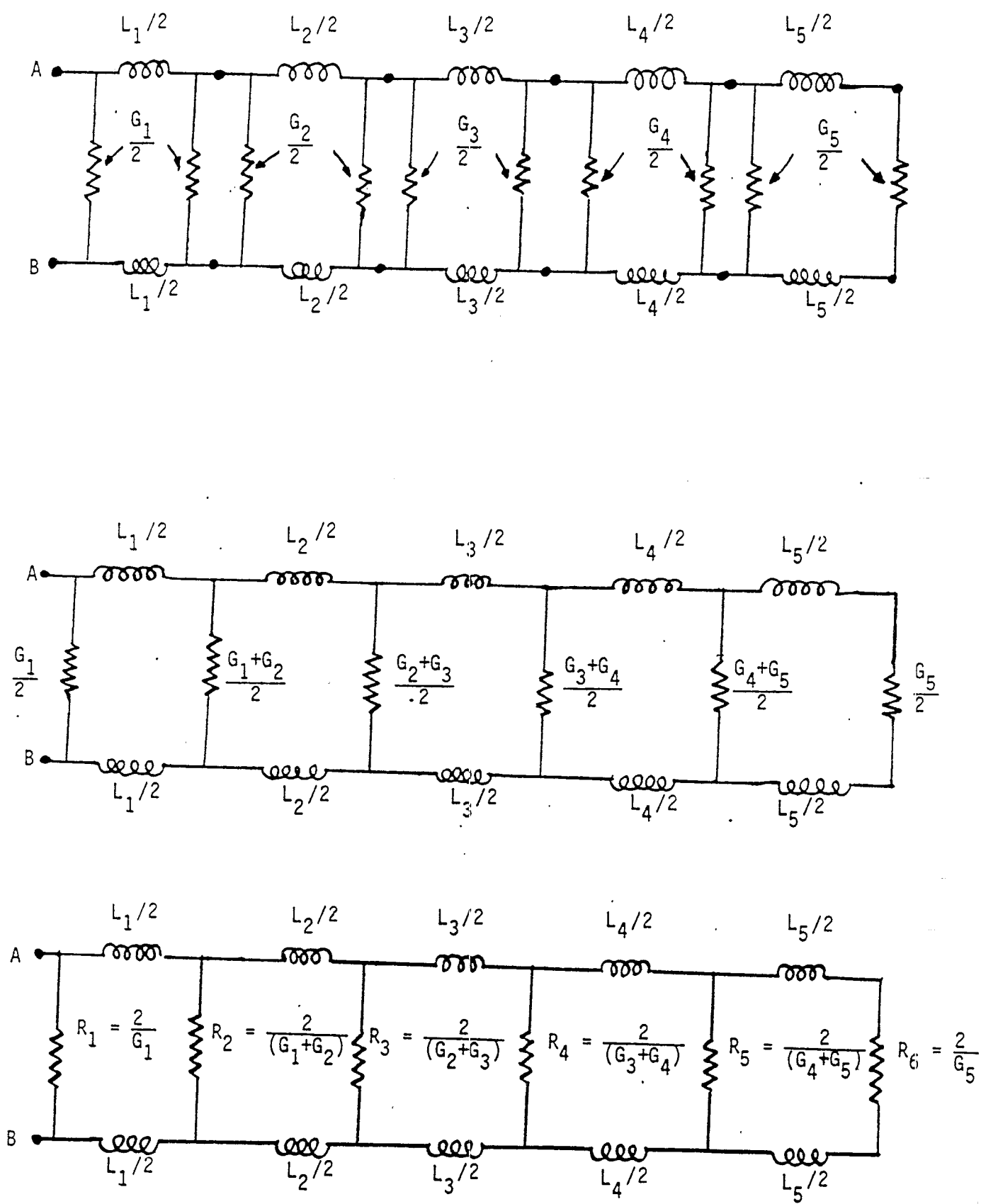


Figure 6.3. Development of the illustrative example network.

It is now recalled that we may choose to have more than one network connected in parallel in order to account for the distributed current path. A choice of 2 parallel networks finally leads to the networks of figure 6.4. Note that, when we have 2 networks in parallel to represent the single network shown at the bottom of figure 6.3, all the series inductances will be doubled and the shunt conductances get halved or shunt resistances get doubled, in order that the overall impedance is preserved. Therefore, the series inductors in one of the two parallel and identical networks are simply L_1, L_2, L_3, L_4 and L_5 and the shunt resistances going from left to right are $4G_1, 4/(G_1+G_2), 4/(G_2+G_3), 4(G_3+G_4), 4/(G_4+G_5)$ and $4/G_5$ respectively. Substituting the values of L_n and G_n for $n = 1$ to 5 from (6.5) leads to the elemental values indicated on one of the two networks in figure 6.4. The other network in figure 6.4 is identical.

Next, we may compare the expected performance of the network with the desired characteristics by comparing the open circuit impedance \tilde{Z}_{L_1} of a 98m line with the input impedance of the network. This comparison can be done on the imaginary axis of the complex s-plane by setting $s = j\omega$. The desired impedance, using (3.3) is given by

$$\tilde{Z}_{L_1}(\omega) = M_c e^{j\theta_c} = f_g \left(\frac{j\omega\mu_0}{\sigma + j\omega\epsilon} \right)^{1/2} \coth\left(\ell_1 \sqrt{j\omega\mu_0(\sigma + j\omega\epsilon)}\right) \quad (6.6)$$

and the network impedance $\tilde{Z}_{AB}^{(n)}$ given by

$$\tilde{Z}_{AB}^{(n)}(\omega) = 2\tilde{Z}_{A_1B_1}^{(n)}(\omega) = 2\tilde{Z}_{A_2B_2}^{(n)}(\omega) \quad (6.7)$$

is readily computed by using basic electrical circuit theory. The results of these calculations are given in tables 6.1 and 6.2, and plotted in figure 6.5. It is seen from figure 6.5 that the impedance comparisons of the continuous case with the network (calculated) is excellent up to about 1 MHz. The deviations above 1 MHz is easily explained by referring to figure 6.1 and observing that the low frequency

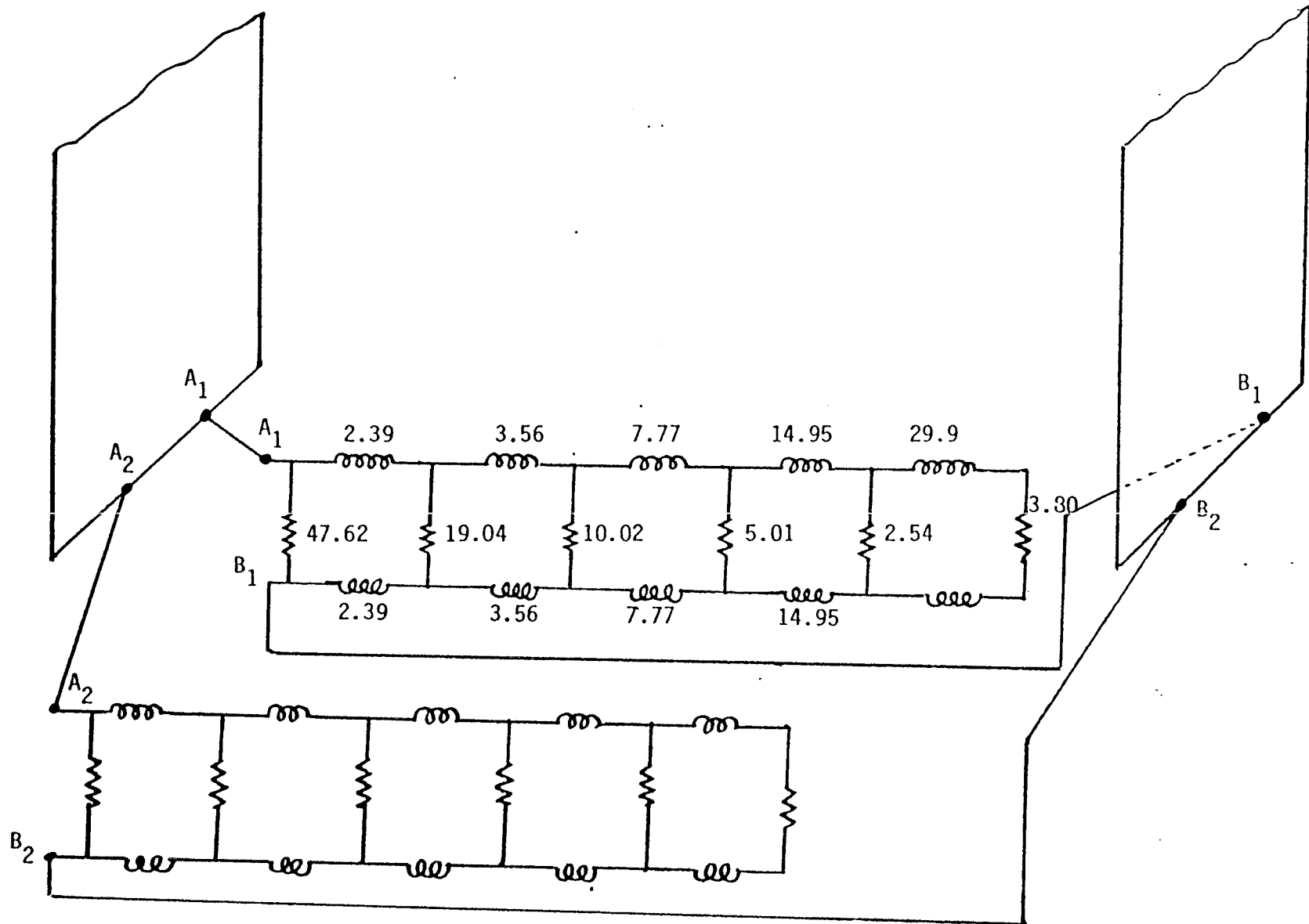


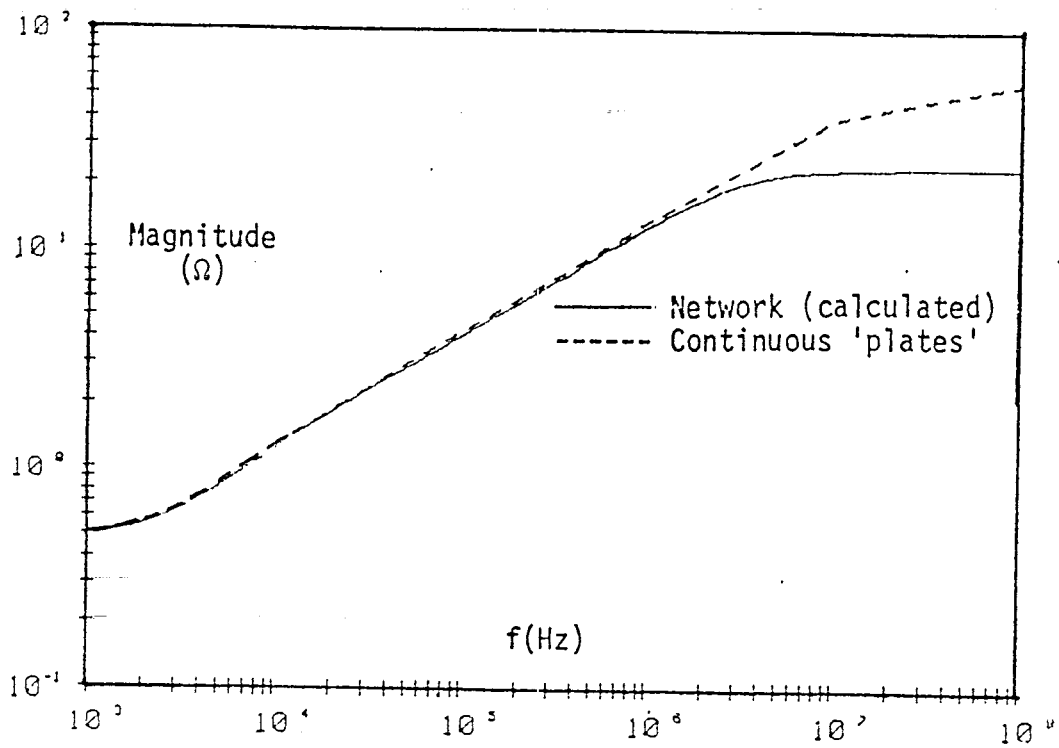
Figure 6.4. Schematic (not the physical lay out) network comprising of two identical parallel networks for the illustrative example. All inductances are in μH and all resistances are in Ω .

f(Hz)	R(Ω)	X(Ω)	M _c (Ω)	θ_c degrees
DC	0.486	0	0.486	0
10 ²	0.486	0.01229	0.4861	1.45
10 ³	0.486	0.1229	0.5012	14.19
10 ⁴	0.895	0.943	1.300	46.5
10 ⁵	2.995	2.995	4.230	45
10 ⁶	9.669	9.203	13.382	43.45
10 ⁷	34.139	20.101	39.618	30.49
10 ⁸	56.195	5.025	56.195	5.11

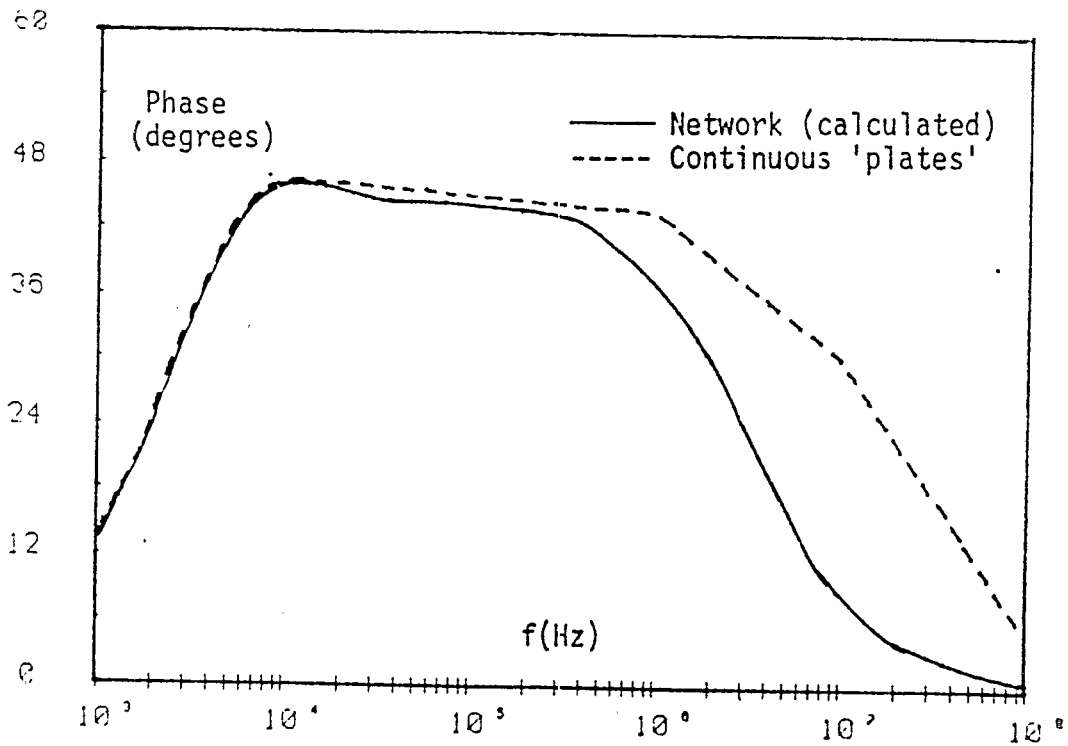
TABLE 6.1. Computation of $\tilde{Z}_{L_1}(\omega)$ of equation (6.6)
subscript c denotes the 'continuous' plate
case $\sigma = 10^{-2}$ S/m, $\epsilon_r = 10$, $l_1 = 98$ m.
Note $R = M_c \cos(\theta_c)$ and $X = M_c \sin(\theta_c)$

f(Hz)	M ^(c) (Ω) 1 network	M _n ^(c) (Ω) 2 networks	θ_n ^(c) degrees
DC	0.962	0.481	0
10 ³	1.003	0.5015	13.53
2 x 10 ³	1.113	0.556	24.7
5 x 10 ³	1.650	0.825	41.29
1.024 x 10 ⁴	2.517	1.258	45.85
1.048 x 10 ⁵	8.305	4.152	44.18
7.56 x 10 ⁵	22.420	11.210	39.01
1.072 x 10 ⁶	26.340	13.170	36.48
1.918 x 10 ⁶	33.850	16.925	30.53
4.865 x 10 ⁶	43.56	21.780	16.81
1.097 x 10 ⁷	46.46	23.230	8.025
4.97 x 10 ⁷	47.26	23.630	1.804
10 ⁸	47.29	23.645	0.898

TABLE 6.2. Computation of the impedance of the network(s)
representing the above continuous line.



(a) Magnitude



(b) Phase

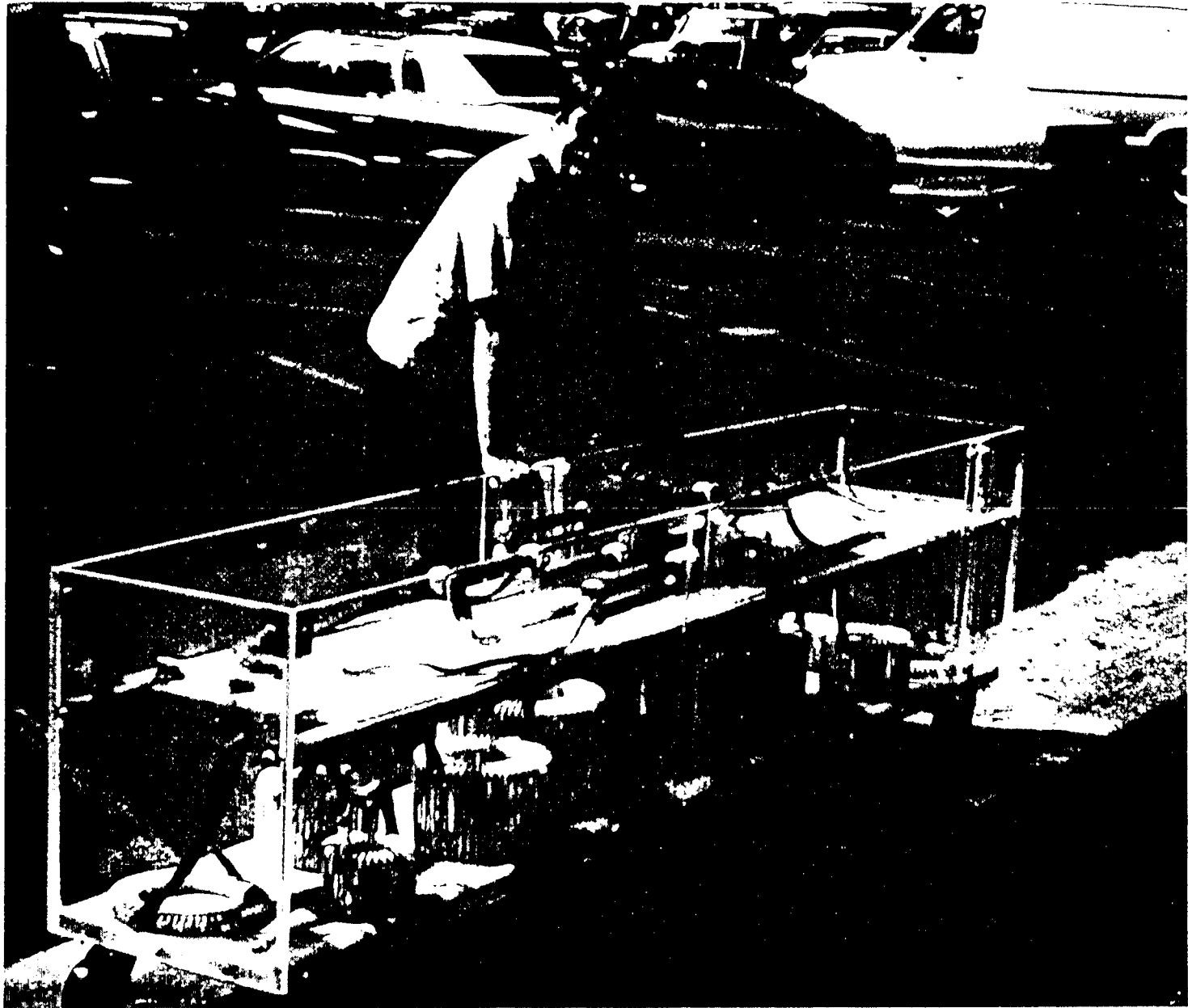
Figure 6.5. Impedance comparison of the continuous case with the network calculations.

approximation used in designing the network breaks down above 1 MHz. The dielectric property of the soil comes into play and can only be accounted in the network by shunt capacitances. This has not been done in the present example. This comparison also shows that having only 5 sections for the 98m length is adequate and the network is not all that lumpy at all.

Next, the two networks shown in figure 6.4 were fabricated using carbon resistors and recently designed [7] low-external-field inductors. The network(s) are shown in figure 6.6. The inductors because of their inherent property can be combined in series/parallel sense without any undesirable interaction. Even inductors in different parts of the circuit also do not have any mutual coupling which is helpful in the present application. The measurements of impedance were done on one of the networks and halved in magnitude for the total network. The results of the measurement are indicated in Table 6.3 and they are compared with the calculated impedance of the network in figure 6.7. It is seen that the network consistently measures somewhat higher magnitude and phase, perhaps due to lead inductances.

To test the above hypothesis that the lead inductances in the measurement could be the cause of the deviations in figure 6.7, these lead inductances are estimated for the experimental configuration during measurement. This configuration is indicated in figure 6.8, where the network housed in a dielectric supporting box is located above a ground plane used as the return conductor. The lead inductance in the experiment L_e is now easily estimated as follows

$$\begin{aligned}
 L_e &\approx \text{length of the network} \times \text{Inductance per unit length} \\
 &\approx 2.79\text{m} \times \left(\frac{\mu_0}{2\pi}\right) \ln\left(\frac{2 \times 0.17}{0.015}\right) \quad (6.8) \\
 &\approx 1.74 \mu\text{H}
 \end{aligned}$$

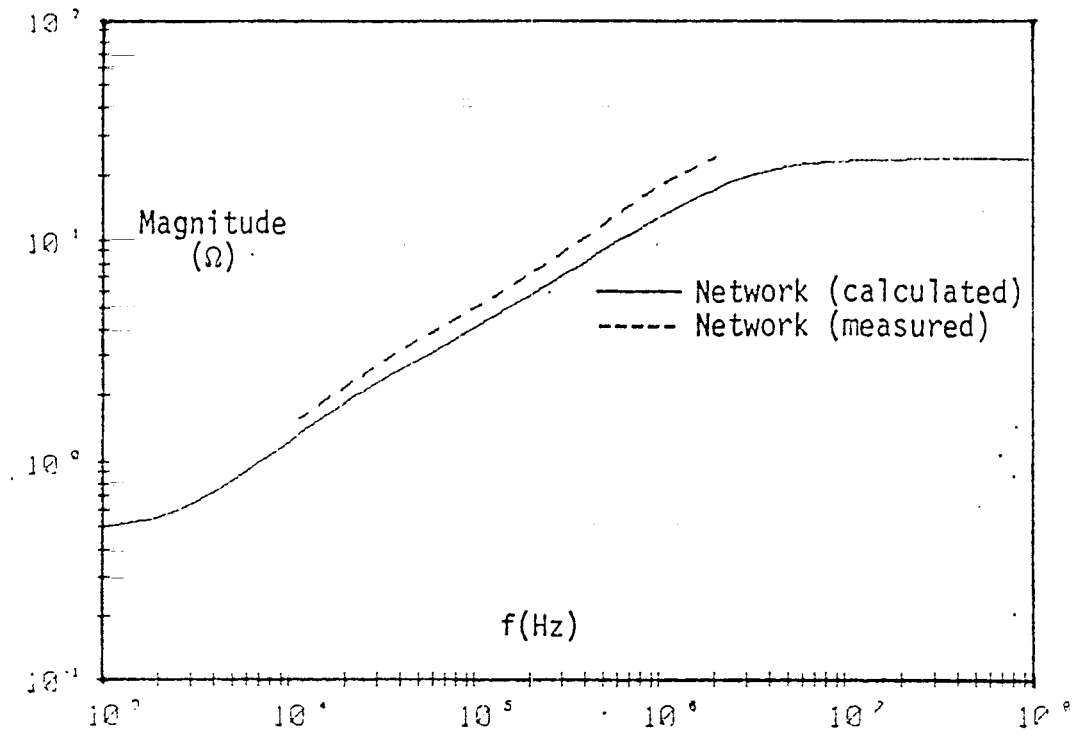


MLA-12, 066

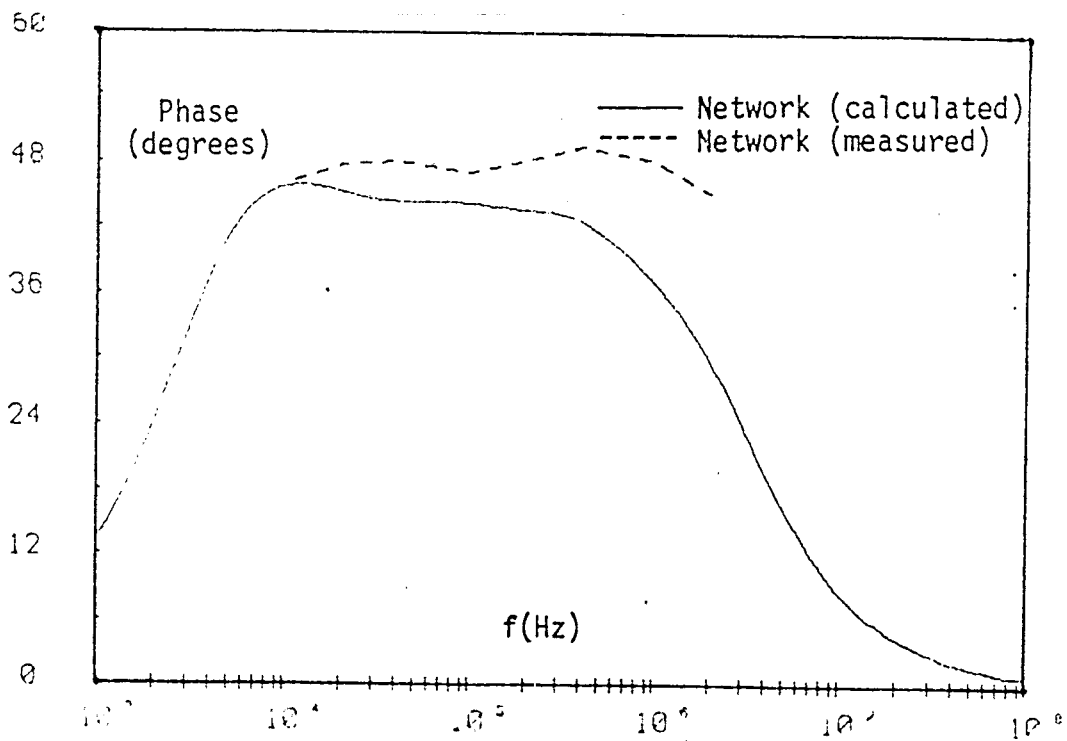
Figure 6.6. Photograph of one of the two identical networks that were fabricated.

f(Hz)	$M^{(m)}(\Omega)$ 1 network	$M^{(m)}(\Omega)$ 2 networks	$\theta(\Omega)$ degrees
10^4	2.9	1.45	48
2×10^4	4.3	2.15	47.8
4×10^4	6.4	3.2	48.1
10^5	10.0	5.0	47.1
2×10^5	14.3	7.15	48.2
4×10^5	21.0	10.5	49.5
10^6	35.7	17.85	48.2
2×10^6	48.4	24.2	45.2

TABLE 6.3. Results of impedance measurement on the network(s).



(a) Magnitude



(b) Phase

Figure 6.7. Impedance comparison of the network (calculated versus measured).

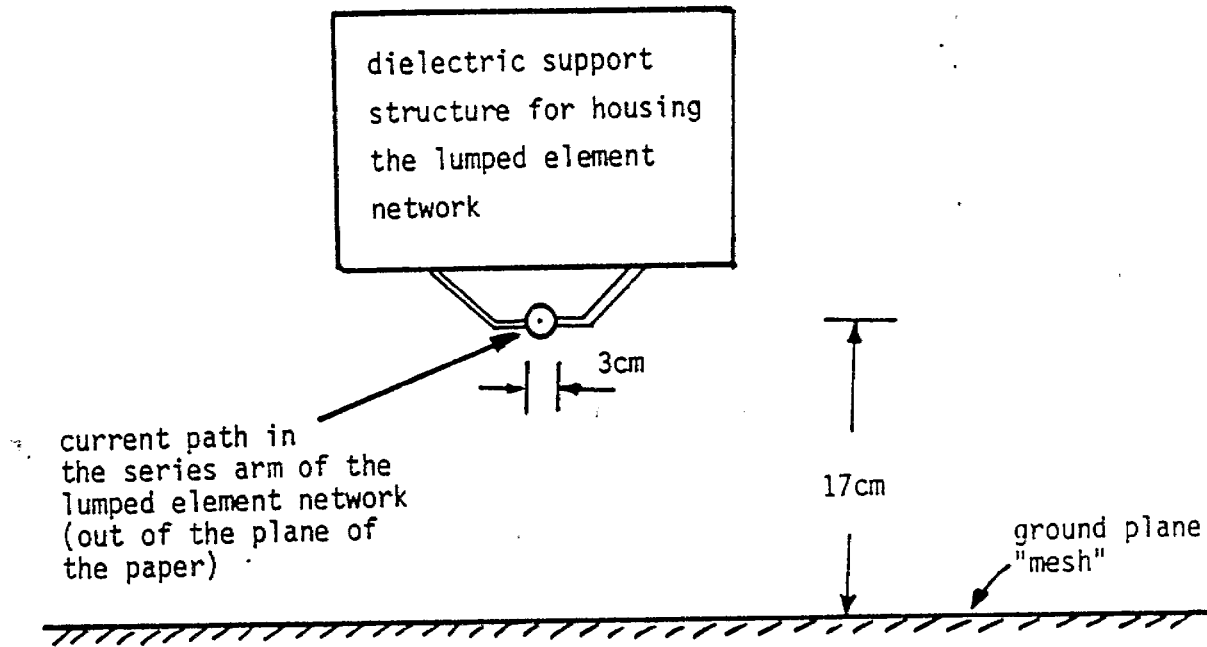


Figure 6.8. Cross-sectional view of the network above a ground plane, as configured during the impedance measurement in the laboratory.

This means, to the calculated impedance of the network (see Table 6.2 and figure 6.5), one should add the above lead inductance and then compare with the experimental results of the network. We therefore have

$$\tilde{Z}_{c\ell} = \tilde{Z}^{(c)} + j\omega L_e/2 = M_{c\ell} e^{j\theta_{c\ell}} \quad (6.9)$$

where

$$\begin{aligned} \tilde{Z}_{c\ell} &= \text{calculated network impedance with lead inductance} \\ \tilde{Z}^{(c)} &= \text{calculated network impedance without lead inductance} \\ &= M_n^{(c)} e^{j\theta_n^{(c)}} \quad (\text{see Table 6.2}) \end{aligned}$$

$\tilde{Z}_{c\ell}$ is now computed and shown in Table 6.4 and is compared with the measured values in figure 6.9.

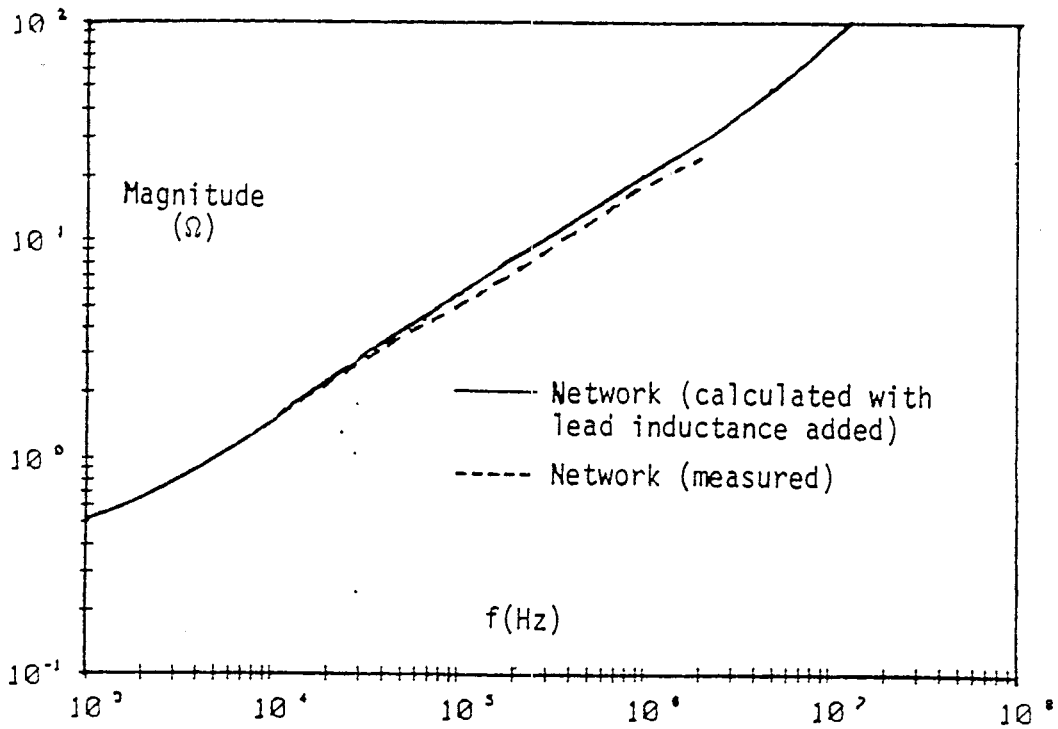
It is seen that when the network impedance calculations are compensated for the presence of the estimated lead inductance, the agreement with measurements is much improved up to about 1 MHz, which is the upper limit for the approximations made. Beyond about the 2 MHz value, the lead inductance is seen to swamp out the network impedance, as one may expect.

The comparison in figure 6.9 suggests the following conclusion, i.e., when the lumped element network is used in practice, one should estimate the unavoidable lead inductance value and its effect may then be accounted by adjusting the initial network elements, via the standard circuit-impedance synthesis procedures.

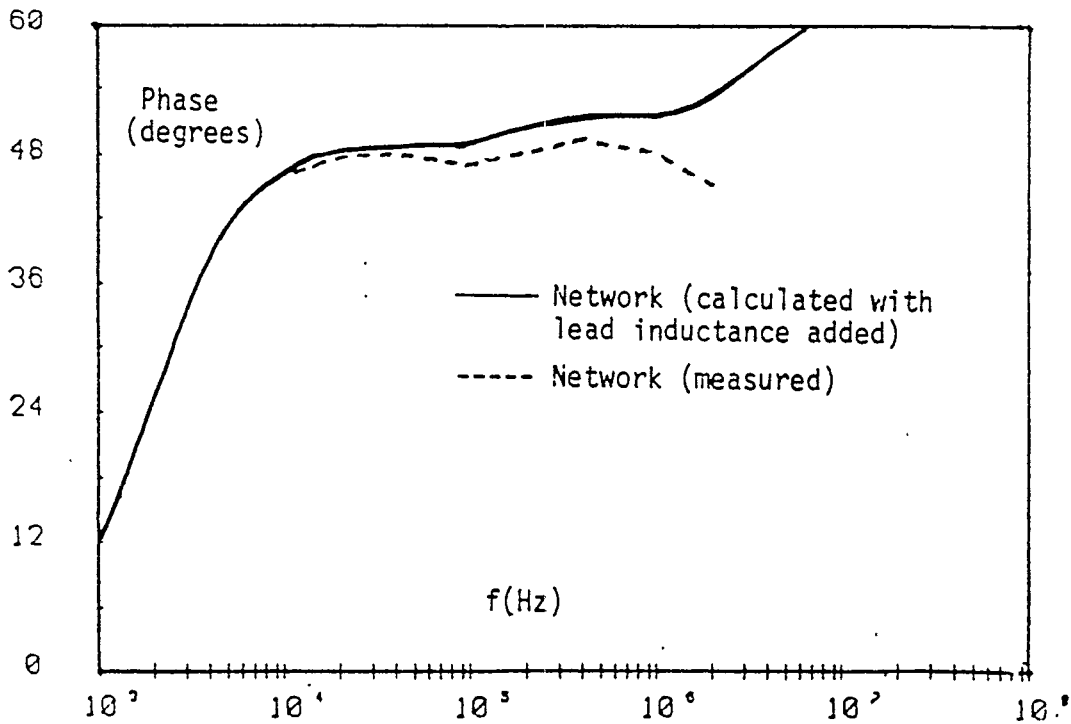
In addition to testing the fabricated networks by themselves in a laboratory, the networks were used in terminating a 2m long transmission line with sand medium. Basically a box containing sand (nominally $\sigma = 10^{-2}$ S/m and $\epsilon_r = 10$) is fabricated. The dimensions of the box as indicated in figure 6.10, are 4m x 8m x 2m. The "buried" transmission line is formed by vertical conductors in the

f(Hz)	$M_{cl}(\Omega)$	θ_{cl} (degrees)
DC	0.481	0
10^3	0.503	14.147
2×10^3	0.560	25.696
5×10^3	0.844	42.694
1.024×10^4	1.297	47.590
1.048×10^5	4.570	49.339
7.56×10^5	14.682	53.609
1.072×10^6	17.308	52.276
1.918×10^6	24.014	52.620
4.865×10^6	38.942	57.630
1.097×10^7	144.766	80.851

TABLE 6.4. Calculated impedance of two identical networks in parallel with the additional estimated lead inductance.

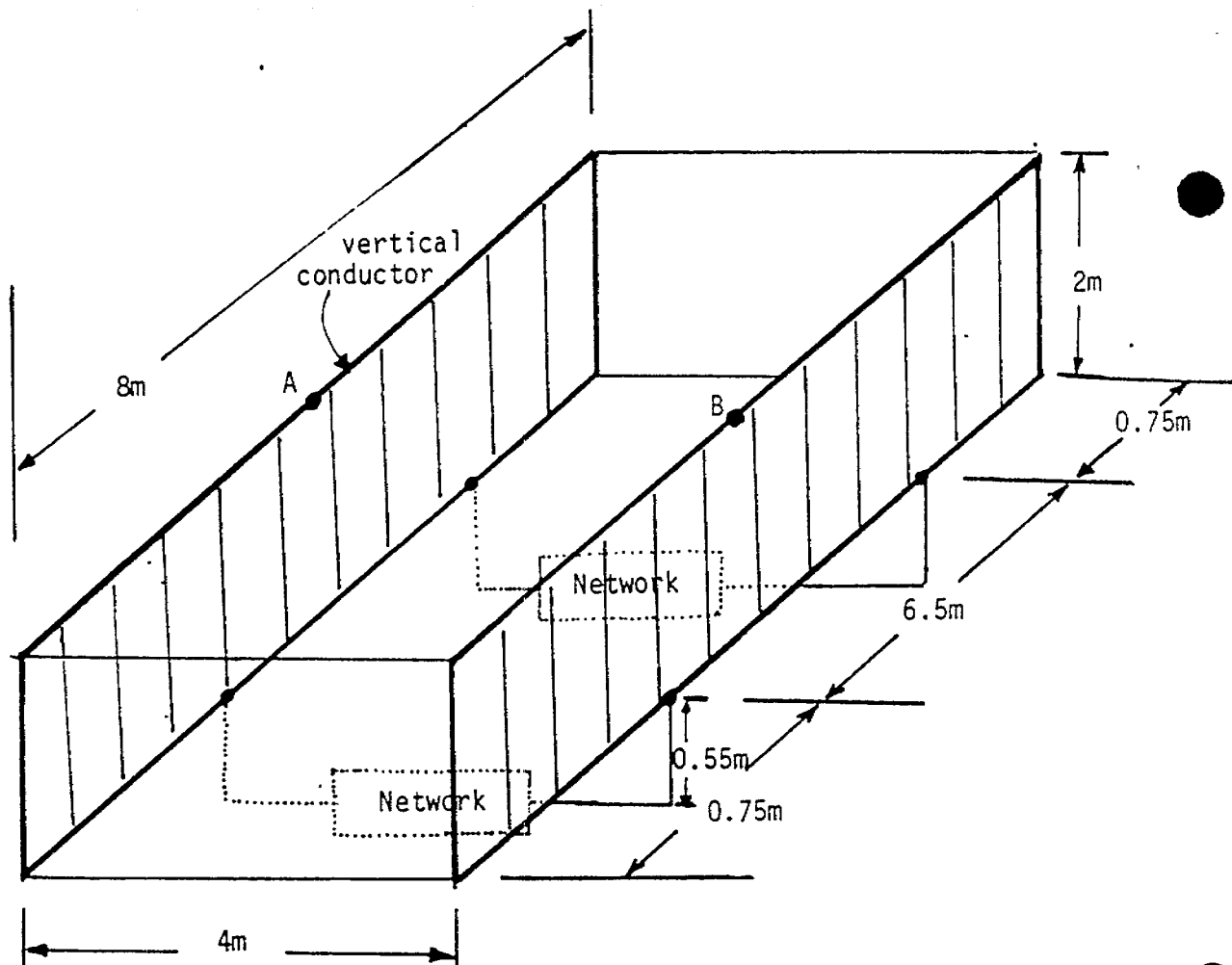


(a) Magnitude

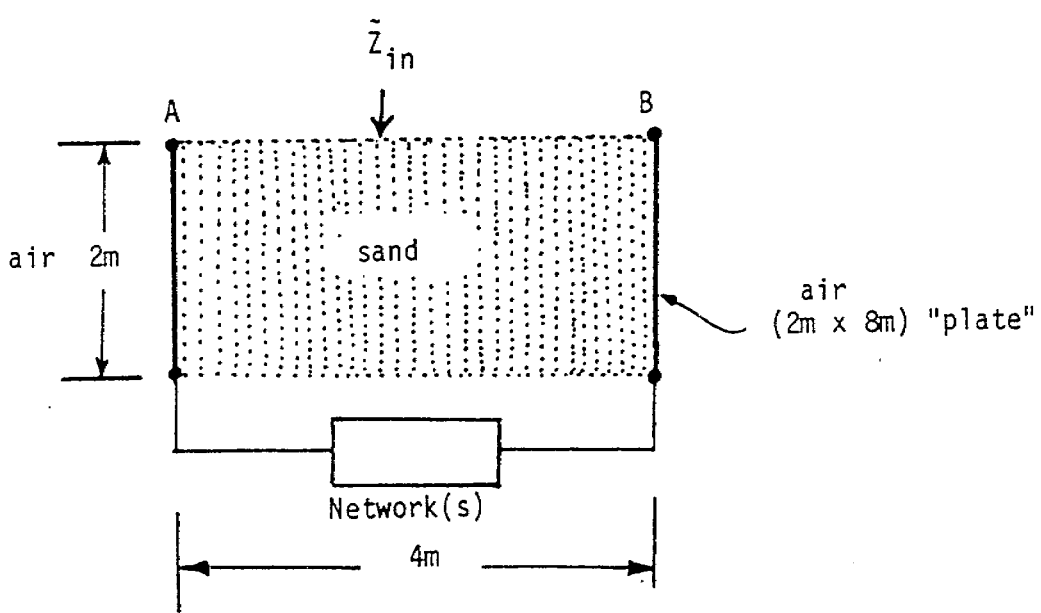


(b) Phase

Figure 6.9. Impedance comparisons of the network (calculated with added lead inductance) versus measured.



(a)



(b)

Figure 6.10. Experimental setup: (a) sand box dimensions, (b) side view indicating the impedance looking into the buried transmission line, for both measurement and calculations.

form of "plates" of size 2m x 8m. The plate separation is 4m. Although the separation to width ratio is 0.5, because of the absence of the sand in the exterior region of the plates, an effective ratio is estimated resulting in an f_g of 0.4764. This value of f_g along with the above mentioned constitutive parameters are then used in calculating the input impedance of the transmission line at the terminal AB, while the 2m network is terminated by the network(s) derived earlier (see figure 6.4). A photograph of one of the two networks used in parallel to terminate the buried 2m transmission line may also be seen in figure 6.6.

Given the configuration of figure 6.10, the input impedance $\tilde{Z}_{in}(s)$ at the terminal AB, is now given by

$$\tilde{Z}_{in}(s) = \tilde{Z}_{L_\infty}(s) \left[\frac{\tilde{Z}_{L_1}(s) + \tilde{Z}_{L_\infty}(s) \tanh(\gamma \ell_0)}{\tilde{Z}_{L_\infty}(s) + \tilde{Z}_{L_1}(s) \tanh(\gamma \ell_0)} \right] \quad (6.10)$$

where $\tilde{Z}_{L_1}(s) \equiv$ the "load" impedance or the combined impedance of the two identical parallel networks. Setting the complex frequency $s = j\omega$, (6.10) becomes,

$$\tilde{Z}_{in}(\omega) = \tilde{Z}_{L_\infty}(\omega) \left[\frac{\tilde{Z}_{L_1}(\omega) + j\tilde{Z}_{L_\infty}(\omega) \tan(k\ell_0)}{\tilde{Z}_{L_\infty}(\omega) + j\tilde{Z}_{L_1}(\omega) \tan(k\ell_0)} \right] \quad (6.11)$$

The above expression has been computed and compared with measured input impedance at the terminal AB. The measured values are listed in Table 6.5 and the comparison is done in figure 6.11. It is noted that the measurement is performed with an impedance analyzer placed in the center, somewhat raised from the top surface of the sand medium. The connections between the impedance meter and the vertical transmission line conductors are achieved by 'plates' (wire meshes in practice) that are approximately triangular in shape, with a narrow edge near the meter and a matching edge of 8m at the other end.

f (Hz)	Magnitude $ \tilde{Z}_{in} \Omega$	Phase θ degrees
10 ⁴	1.6	50
2 x 10 ⁴	2.5	50.3
4 x 10 ⁴	3.7	50
10 ⁵	6.1	49.3
2 x 10 ⁵	8.9	50.3
4 x 10 ⁵	13.6	50.8
10 ⁶	23.8	44
2 x 10 ⁶	31.7	34.6
10 ⁷	62.0	35.4

TABLE 6.5. Measured input impedance at terminal AB of figure 6.10.

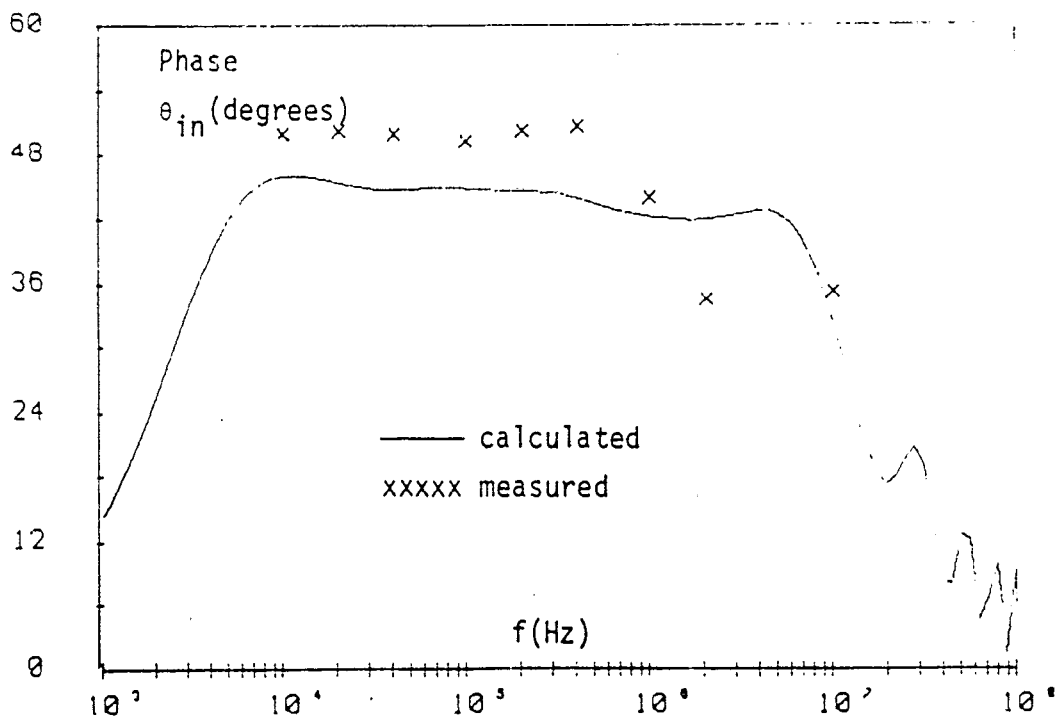
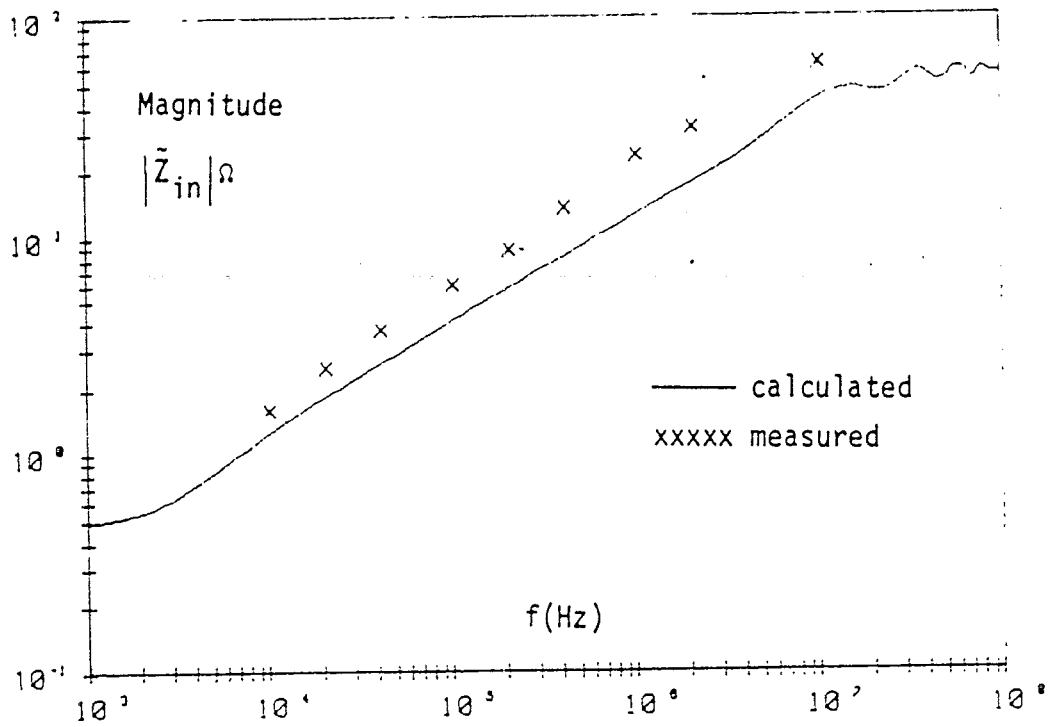


Figure 6.11. Comparison of the calculated and measured input impedance.

In figure 6.10, it is seen that the agreement is seen to be fair up to about 10 MHz, although the measured magnitude is higher than the calculated values. The reasons for this mainly lie in the lead inductances at the top (connections from the impedance meter to the transmission line conductors) and bottom (connections from the transmission line conductors to the networks) of the transmission line. There could also be deviations in the values of σ and ϵ_r for the sand from what have been used in the computation. If suitable corrections are made for these lead inductances (impedances in general), the agreement between the measured and calculated impedances should improve. Note also the oscillations in the magnitude of the calculated input impedance, corresponding roughly to the resonance of the 2m buried transmission line itself. This is unavoidable, but it is of sufficiently small magnitude, so that simulation fidelity is not strongly affected.

VII. SUMMARY

This note has addressed the problem of designing a lumped-element network to represent all or a portion of a buried transmission line formed by two vertical perfectly conducting "plates". The network emulates the impedance of a long section of an open circuited buried line. Such an impedance equality is accomplished by dividing the transmission line into a suitable number of sections, each of which is then replaced by its incremental-length model. The individual model consists of series inductances and shunt conductances and shunt capacitances as well. The shunt capacitance elements are negligible at low frequencies where the conduction current in the soil medium dominates over the displacement current. Finally, one arrives at a cascaded section of several incremental model networks. An illustrative example has been demonstrated through design, fabrication and testing. The alternate current paths at the termination port have also been discussed, since it impacts how the network(s) is (are) physically connected to the vertical conductors in maintaining the fidelity of the magnetic fields. The network also takes advantage of a recently designed way of fabricating field-containing inductors.

In evaluating this concept, the open circuit impedance of a section of buried transmission line is compared with the calculated network impedance, and the agreement is seen to be excellent in the range of frequencies where the low-frequency approximation is valid. This approximation has been made in the design of the network. In evaluating the network, the measured impedance is compared with the calculated impedance of the network. Although the measurement configuration attempts to minimize all undesirable lead and inter-element wire inductances by the use of braids and a ground plane for the return conductor, it has been observed that some amount of additional lead inductances is still present in the network. A procedure to compensate for the unavoidable lead inductances, by adjusting the values of perhaps the initial network elements has been demonstrated to be worthwhile.

In terminating this note (the pun is intended), it is noted that this concept is expected to prove useful in EMP simulation development.

REFERENCES

1. C.E. Baum, "EMP Simulators for Various Types of Nuclear EMP Environments: An Interim Categorization," Sensor and Simulation Note 240, January 1978 and Joint Special Issue on the Nuclear Electromagnetic Pulse, IEEE Trans. on Antennas and Propagation, January 1978, pp 35-53, and IEEE Trans. on Electromagnetic Compatibility, February 1978, pp 35-53.
2. C.E. Baum, "A Transmission Line EMP Simulation Technique for Buried Structures," Sensor and Simulation Note 22, June 1966.
3. C.E. Baum, "The Capacitor Driven Open circuited Buried-Transmission-Line Simulator," Sensor and Simulation Note 44, June 1967.
4. R.W. Latham and K.S.H. Lee, "The Buried Transmission Line Simulator With an Inductive Energy Source," Sensor and Simulation Note 50, April 1968.
5. D.W. Milligan, "The Buried Transmission-Line Simulator Driven by Multiple Capacitive Sources and an Inductive Source," Sensor and Simulation Note 76, March 1969.
6. C.E. Baum, T.K. Liu and F.M. Tesche, "On the Analysis of General Multiconductor Transmission-Line Networks," Interaction Note 350, November 1978.
7. Y.G. Chen, R. Crumley, C.E. Baum and D.V. Giri, "Field-Containing Inductors," Sensor and Simulation Note 287, July 1985.